SAND REPORT

SAND2002-2597
Unlimited Release
Printed August 2002

Three-Dimensional Wind Field Modeling: A Review

Gregory F. Homicz

Prepared by
Sandia National Laboratories
Albuquerque, New Mexico 87185 and Livermore, California 94550

Sandia is a multiprogram laboratory operated by Sandia Corporation, a Lockheed Martin Company, for the United States Department of Energy under Contract DE-AC04-94AL85000.

Issued by Sandia National Laboratories, operated for the United States Department of Energy by Sandia Corporation.

Available to DOE and DOE contractors from
U.S. Department of Energy
Office of Scientific and Technical Information
P.O. Box 62
Oak Ridge, TN 37831

Telephone: (865)576-8401
Facsimile: (865)576-5728
E-Mail: reports@adonis.osti.gov
Online ordering: http://www.doe.gov/bridge

Available to the public from
U.S. Department of Commerce
National Technical Information Service
5285 Port Royal Rd
Springfield, VA 22161

Telephone: (800)553-6847
Facsimile: (703)605-6900
E-Mail: orders@ntis.fedworld.gov
Online order: http://www.ntis.gov/ordering.htm

SAND2002–2597
Unlimited Release
Printed August 2002

Three-Dimensional Wind Field Modeling: A Review

Gregory F. Homicz
Thermal/Fluid Computational Engineering Sciences Department
Sandia National Laboratories
P. O. Box 5800
Albuquerque, New Mexico 87185-0835

Abstract

Over the past several decades, the development of computer models to predict the atmospheric transport of hazardous material across a local (on the order of 10s of km) to mesoscale (on the order of 100s of km) region has received considerable attention, for both regulatory purposes, and to guide emergency response teams. Wind inputs to these models cover a spectrum of sophistication and required resources. At one end is the *interpolation/ extrapolation* of available observations, which can be done rapidly, but at the risk of missing important local phenomena. Such a model can also only describe the wind at the time the observations were made. At the other end are sophisticated numerical solutions based on so-called Primitive Equation models. These *prognostic* models, so-called because in principle they can forecast future conditions, contain the most physics, but can easily consume tens of hours, if not days, of computer time. They may also require orders of magnitude more effort to set up, as both boundary and initial conditions on all the relevant variables must be supplied. The subject of this report is two classes of models intermediate in sophistication between the interpolated and prognostic ends of the spectrum. The first, known as *mass-consistent* (sometimes referred to as *diagnostic*) models, attempt to strike a compromise between simple interpolation and the complexity of the Primitive Equation models by satisfying only the conservation of mass (continuity) equation. The second class considered here consists of the so-called *linear* models, which purport to satisfy both mass and momentum balances. A review of the published literature on these models over the past few decades was performed. Though diagnostic models use a variety of approaches, they tend to fall into a relatively few well-defined categories. Linear models, on the other hand, follow a more uniform methodology, though they differ in detail. The discussion considers the theoretical underpinnings of each category of the diagnostic models, and the linear models, in order to assess the advantages and disadvantages of each. It is concluded that diagnostic models are the better suited of the two for predicting the atmospheric dispersion of hazardous materials in emergency response scenarios, as the linear models are only able to accommodate gently-sloping terrain, and are predicated on several simplifying approximations which can be difficult to justify *a priori*. Of the various approaches used in diagnostic modeling, that based on the calculus of variations appears to be the most objective, in that it introduces the fewest number of arbitrary parameters. The strengths and weaknesses of models in this category, as they relate to the activities of Sandia's Nuclear Emergency Support Team (NEST), are further highlighted.

Acknowledgement

The author wishes to thank Dr. Bruce Boughton (Org. 05800) for suggesting this project, and the Nuclear Emergency Support Team (NEST) for their support during this effort. He would also like to express his appreciation to John Fulton and William Wente (Org. 5817), and Drs. John Brockmann and Charles Hickox (Org. 9117), for their comments on an early draft of this report, which led to a much improved manuscript.

Table of Contents

Intentionally Left Blank

List of Figures

Intentionally Left Blank

Nomenclature

c	determines weighting assigned to various points in Liu and Goodin's (1976) modified Point-Iterative scheme (*cf.* Fig. 1); dimensionless
D_{ijk}	three-dimensional divergence; [sec^{-1}]
E	functional defined by Eq. (28); [m^3]
f_{ij}	parameter used in Liu and Goodin's (1976) modified Point-Iterative scheme to preserve data at or near observation stations ($f_{ij} = 0$), or allow the flow to adjust without constraint ($f_{ij} = 1$); dimensionless
F	a perturbation field (*e.g.*, velocity or pressure) in the linearized analysis; dimensions arbitrary
F	Fourier decomposition (either transform or discrete spectrum) of F in linearized analysis; dimensions arbitrary
FD	Finite-Difference
FE	Finite-Element
Fr	Froude number, $U_\infty/(Nh)$; dimensionless
g	gravitational acceleration; [m/sec^2]
h	characteristic height of terrain features (*cf.* Fig. 4); [m]
$h(x, y)$	local surface height above some reference level; [m]
H_c	upstream height of the critical streamline dividing flow that passes around an obstacle from that passing over it (*cf.* Eq. (41)); [m]
$H(x, y, t)$	height above reference level of the top of the computational domain (typically the top of the boundary layer, or the base of an elevated temperature inversion); [m]
ΔH	local height of the computational domain, $H(x, y, t) - h(x, y)$; [m]
i	$\sqrt{-1}$ (in *Appendix A*); dimensionless
i, j, k	integer indices in the (x, y, z) directions, respectively; dimensionless
ILU	Incomplete Lower/Upper triangular factorization
k	wavenumber in Fourier decomposition (*Appendix A*); [m^{-1}]
l	depth of inner region in linearized model (*cf.* Fig. 4); [m]
L	characteristic horizontal scale of terrain features in linearized model (*cf.* Fig. 4); [m]
L	horizontal extent of flat plain surrounding region of interest in linearized model (*cf.* Fig. 5); [m]

L_R	horizontal extent of region of interest in linearized model (*cf.* Fig. 5); [m]
L_T	horizontal extent of transition zone surrounding region of interest in linearized model (*cf.* Fig. 5); [m]
m	index in Fourier series in *Appendix A*; dimensionless
N	Brunt-Väisälä frequency, $[(g/\theta)(\partial\theta/\partial z)]^{1/2}$; [sec^{-1}]
S	terrain-induced speedup factor, U_{max}/U_∞; dimensionless
SOR	Successive Over-Relaxation
SSOR	Symmetric Successive Over-Relaxation
SST	stair-step terrain representation of the topography (*cf.* p. 27)
TFC	terrain-following coordinate mapping of the topography (*cf.* p. 5)
U_∞	uniform background velocity field; [m/sec]
$U_0(z)$	oncoming velocity profile in linearized model (*cf.* Fig. 4); [m/sec]
u, v, w	components of mean wind along x, y, z respectively; [m/sec]
u_i, v_i, w_i	interpolated, or initial guess, wind field; [m/sec]
u', v', w'	perturbation velocities along x, y, z respectively, in the linearized model, *cf.* Eq. (48).
$\pm\bar{u}_{i,j}$	corrections added to $u^n_{i\pm1,j}$ in Point-Iterative scheme to enforce $\delta^{n+1}_{ij} = 0$; [m/sec]
$\pm\bar{v}_{i,j}$	corrections added to $v^n_{i,j\pm1}$ in Point-Iterative scheme to enforce $\delta^{n+1}_{ij} = 0$ [m/sec]
$\pm\hat{u}_{ij}$	corrections added to $u^n_{i,j\pm1}$ in Point-Iterative scheme to enforce $\omega^{n+1}_{ij} = \omega^0_{ij}$ [m/sec]
$\pm\hat{v}_{ij}$	corrections added to $v^n_{i\pm1,j}$ in Point-Iterative scheme to enforce $\omega^{n+1}_{ij} = \omega^0_{ij}$ [m/sec]
x, y, z	right-handed Cartesian coordinate system with x and y lying in the horizontal plane, and z pointing upward; [m]
x_1, x_2	bounding values in the x-direction of the computational domain; [m]
y_1, y_2	bounding values in the y-direction of the computational domain; [m]
z_1, z_2	bounding values in the z-direction of the computational domain; [m]
z_0	characteristic roughness length of the terrain; [m]
z_{in}	scaled vertical coordinate used in inner region of linearized model; [m]
z_{out}	scaled vertical coordinate used in outer region of linearized model; [m]

Greek Symbols

α	the ratio (α_1/α_2); dimensionless
α_1, α_2	Gauss precision moduli, or weighting factors, applied to the horizontal and vertical components of the wind, respectively (*cf.* Eq. (28)); [$(m/sec)^{-1}$]
α_u, α_v, α_w	Gauss precision moduli, or weighting factors, applied to the *u*, *v*, and *w* components of the wind, respectively (*cf.* Eq. (45)); [$(m/sec)^{-1}$]
β	the fraction of the total velocity correction in Liu and Goodin's (1976) modified Point-Iterative scheme applied on each iteration at the "$\triangle$" points in Fig. 1; dimensionless
γ_{ij}	weight factor that controls the degree to which original data are preserved by the smoothing filter in Goodin, *et al*.'s (1980) Hybrid approach (*cf.* Eq. (20)); dimensionless
δ	horizontal divergence, defined in Eq. (8); [sec^{-1}] also used to represent boundary layer thickness in linearized model (*cf.* Fig. 4); [m]
$\delta(\ldots)$	variation of the quantity that follows; same dimensions as (…)
η	the fraction of the total velocity correction in Liu and Goodin's (1976) modified Point-Iterative scheme applied on each iteration at the "$\circ$" points in Fig. 1; dimensionless
λ	Lagrange multiplier in Eq. (28); [sec]
θ	potential temperature; [°K]
ρ	density; [kg/m^3]
σ	elevation-based terrain-following vertical coordinate (TFC) defined in Eq. (3); dimensionless
ω	vertical component of vorticity, defined in Eq. (9); [sec^{-1}]

Intentionally Left Blank

1. INTRODUCTION

The Nuclear Emergency Support Team (NEST) at Sandia National Laboratories is tasked with responding to situations involving the accidental or deliberate release of radiological, biological, or chemical hazards into the atmosphere. The transport of such material by the atmosphere is heavily dependent on both the mean and fluctuating (turbulent) components of the wind. Among the tools NEST has at its disposal are the Explosive Release Atmospheric Detonation (ERAD) code (Boughton and DeLaurentis (1992)), for modeling the dispersion of radioactive material released by a high explosive (*i.e.*, chemical) detonation, and AIRRAD (Sagartz (1997)), which predicts radioactive fallout patterns resulting from a nuclear detonation. Both ERAD and AIRRAD require as input a three-dimensional (3D) wind field over the entire domain of interest, consisting of the mean wind components *u*, *v*, and *w* defined on a Cartesian grid.

Currently both ERAD and AIRRAD use a simple *interpolated* wind field. This is created from whatever observations are available by interpolating between (or extrapolating from) those observations onto the 3D lattice of grid points, using weight factors that typically vary as the inverse square of the horizontal distance between the data and grid points. (A comparison between this and other interpolation schemes can be found in Goodin, *et al.* (1979).) Interpolated wind fields are easily and quickly generated, an important consideration when one is operating in the field, and "real-time" predictions may be necessary.

One problem with using such an interpolated field is that in general it will not satisfy the equation representing conservation of mass, often referred to as the continuity equation. As noted by Sherman (1978), for flows over scales on the order of 10s to 100s of km, the density ρ may reasonably be assumed constant, in which case the continuity equation reduces to simply:

$$\nabla \cdot \vec{u} = 0 \tag{1}$$

Note that this equation is already linear, with no further approximation needed. The observations themselves will invariably contain some error, and the interpolation procedure applied to them, oblivious as it is to any kinematic restrictions, will introduce further errors of its own. Hence it would be extremely fortuitous if the interpolated wind field did not violate Eq. (1) by retaining a nonzero divergence at most points in the flow. Positive and negative values of the divergence can be interpreted physically as sources and sinks of mass, respectively. The presence of these sources and sinks may significantly contaminate the resulting predictions of hazardous material transport. A second problem with the use of interpolated winds is that they make no correction for terrain effects—the flow is as likely to go through an obstacle, such as a mountain, as it is to pass around or over it.

In an ideal world, a full (nonlinear) Primitive Equation model would be used to predict the wind field, including the influence of topographic changes, if any. However, such models require considerably more computer resources as compared with a simple interpolated wind field, and may take several hours, if not days, for a complete solution. They can also require more detailed information to set up than is typically available. This makes them impractical for applications such as those encountered by NEST, where codes are typically deployed on laptop PCs, and quick turnaround is essential.

This report reviews the published literature on two intermediate classes of wind models which have been developed over the past several decades, and which strike an attractive compromise between physical fidelity and run time. The first consists of the so-called *mass-consistent* or *diagnostic* models, which use the interpolated field as input to an algorithm which makes corrections to ensure that the surface wind is parallel to the underlying terrain, and that Eq. (1) is satisfied at each grid point as well. Unlike prognostic codes, diagnostic models cannot strictly be used as forecasting tools, as Eq. (1) does not contain any temporal derivatives. Nevertheless, their predictions are frequently assumed to persevere sufficiently long so that useful results concerning the spread of the contaminant can be obtained. Diagnostic models are discussed in §2, which follows.

The second class consists of the *linear* or *linearized* models, which in addition to the continuity equation, attempt to solve the momentum conservation equations as well. They do not rely on an interpolated field as their starting point, but rather perform a small-perturbation analysis about an assumed oncoming flow. The steady-state form of the equations is solved, so that again only the flow at the current instant can be studied, not its evolution with time. This class of models is described in §3. Finally, §4 summarizes the findings, and draws conclusions as to which of the models is most appropriate for use in the type of applications encountered by the NEST group at Sandia.

2. DIAGNOSTIC MODELS

As noted in the Introduction, *diagnostic* or *mass-consistent* models attempt to adjust the interpolated wind field so that Eq. (1), the continuity equation for incompressible flow, is satisfied at each grid point, and there is no throughflow at the surface. This section summarizes the results of a literature review on this subject covering the period from approximately 1977 to mid-2001. Relevant publications were identified by electronically searching the Science Citation Index of the Institute for Scientific Information® using the Web-based SciSearch® at LANL[†] application. The index covers over 4,000 journals in 100+ scientific disciplines, and allows the user to search via Author, Title, and/or Abstract keywords. The most salient papers that resulted, including some prior to 1977, are listed beginning on p. 53, sorted alphabetically by first author. The present author apologizes for any significant omissions—such a list is inevitably incomplete, and even if it were not, would no doubt become so within a short time. Space considerations—not to mention the reader's patience—prohibit a discussion of every entry. Rather, the intent is to focus on those that made meaningful contributions to the subject, or provided illuminating comparisons between different approaches.

In an earlier study, Kitada, *et al.* (1983) found that the then-available diagnostic models fell into four broad categories, which they termed Direct-Differencing, Point-Iterative, Hybrid, and Variational Calculus. This categorization remains useful today. Table 1 lists each category in a separate column, with examples of each type listed in (more or less) chronological order below the appropriate heading. Again, the chronology may not be quite accurate, as it was not always clear when a particular model was first developed; for each model, an attempt has been made to reference the latest information available.

Each of §2.1 through §2.4 that follow will discuss a separate category from Table 1, including some discussion of its theoretical basis, and its advantages and disadvantages. To maintain some sense of continuity, an effort has been made to use a consistent notation throughout the report. The discussion will alert the reader to cases where the nomenclature differs from that used in the original source.

[†]Licensed access to SciSearch at LANL® through the Sandia Restricted Network (SRN) is available at the following URL: `http://scisearch2.lanl.gov/sandia/sci.html`

Table 1: Morphology of Diagnostic Wind Models

DIRECT–DIFFERENCING	POINT–ITERATIVE	HYBRID	VARIATIONAL CALCULUS
Reynolds, *et al.* (1973)	Endlich (1967); SST	Goodin, *et al.* (1980); TFC[b]	Sasaki (1958, 1970)
Peters & Jouvanis (1979)	Liu & Goodin (1976); SST	**DIMCOR** Giarola, *et al.* (1995); SST[a]	**MASCON** Dickerson (1978); 2D, SST[a]
Carmichael & Peters (1980)	Endlich (1984): TFC	**CALMET** Scire, *et al.* (2000); TFC[b]	**MATHEW** Sherman (1978) part of ARAC/LLNL; 3D ext. of MASCON; SST[a]
Anderson (1971)	Ludwig, *et al.* (1991)	**TAMOS** Pechinger, *et al.*(2001) Stohl, *et al.* (1997) TFC[b]	**NOABL** Traci, *et al.* (1978); either SST[a] or TFC[b]
Liu and Yocke (1980)			**COMPLEX** Bhumralkar, *et al.* (1980) Endlich, *et al.* (1982); TFC[b]
			ATMOS1 Davis, *et al.* (1984)/LANL, TFC[b]
			MINERVE/SWIFT Geai (1987) Sontowski, *et al.*(1994,1995); part of HPAC; TFC[b]
			Barnard, *et al.* (1987)
			NUATMOS Ross, *et al.* (1988, 1991) ext. of ATMOS1; TFC[b]
			CONDOR, **REDBL** Moussiopoulos, *et al.* (1986, 1988) TFC[b]
			Mathur and Peters (1990)
			WIND04 Venkatesan *et al.* (1996)
			MEM3D Montero, *et al.* (1998) unstructured, FE sol'n.
			Harada, *et al.* (2000)

a. Stair-Step Terrain using "blocked" cells
b. Terrain-Following Coordinates

2.1 Direct-Differencing

The Direct-Differencing approach is the simplest of all the methods, and is typically used when no information is available for the vertical component of the wind. We will denote the initial fields of the two horizontal components by u_i and v_i, which are assumed known throughout the domain of interest; they may result from the interpolation of whatever observations are available, or simply a good initial guess. Equation (1) may be written in Cartesian coordinates as:

$$\frac{\partial w}{\partial z} = -\left(\frac{\partial u_i}{\partial x} + \frac{\partial v_i}{\partial y}\right) \tag{2}$$

Since the "horizontal divergence" on the right-hand side is a known function, this can be viewed as a single equation for the one unknown, *w.* The single boundary condition required is that of no throughflow at the surface, $z = h(x, y)$, which for relatively flat terrain is simply $w = 0$. Thus, if the domain is overlaid with a lattice of Cartesian grid points, this equation can be approximated in terms of finite differences, and the solution for *w* marched upward in *z*. As *the horizontal components are left unchanged*, the mass balance at any grid point is independent of that at neighboring points. Hence no iterations are required, and one pass through the field is all that is required to enforce Eq. (1) everywhere. The final 3D wind field is given by $u = u_i$, $v = v_i$, and *w* as just described.

Equation (2) is useful primarily for terrain that is flat, or nearly so. However, correction of the velocity field so as to satisfy Eq. (1) is most important for complex terrain. The use of Eq. (2) in such situations is problematic because the surface at which the boundary condition must be applied is now highly irregular, and no longer coincides with a constant value of one of the coordinates. One can try and model such surface variations with a Cartesian grid in a "stair-step" manner, by starting with a rectangular parallelepiped of cells, and then manually blocking out those cells that lie below the surface. Within such cells the velocity components are all frozen at zero. As one might imagine, this leads to a very crude—and hence inaccurate—representation of the surface unless very fine grid cells are used vertically. The latter can lead to excessive computer time.

A more elegant solution is the use of a so-called *terrain-following* coordinate (TFC) system[†], such as that used by Reynolds, *et al.* (1973). They retain *x* and *y* as horizontal coordinates, but transform *z* to a terrain-following coordinate:

$$\sigma = \frac{z - h(x, y)}{H(x, y, t) - h(x, y)} \tag{3}$$

where *h* is the surface height above some reference level, and *H* is the corresponding height of the top of the domain. The latter is typically placed at the top of the boundary layer, or at the base of an elevated temperature inversion. Reynolds, *et al.* actually use the symbol ρ rather than σ, but we will use the latter so as not to confuse it with the density, and because σ is the notation most often used in the literature. Note however, that the σ defined in Eq. (3) is purely a function

[†]In the Computational Fluid Dynamics (CFD) community, these are often called body-fitted, or body-conformal coordinates.

of topography, and as such should not be confused with the pressure-based vertical coordinate of the same name often used in meteorological models (*e.g.*, Grell, *et al.* (1994)). The above transformation maps the bottom and top of the domain to $\sigma = 0$ and 1, respectively. Terrain-following coordinates are used in several mass-consistent models (*cf.* Ratto, *et al*. (1994)), not just those based on Direct-Differencing, as reflected in Table 1. Although the domain in *physical* (*x, y, z*)-space is highly irregular near the surface, in *computational* (*x, y,* σ)-space it is a simple rectangular parallelepiped, and the boundary condition maps to $\dot{\sigma} = 0$ on the surface $\sigma = 0$. If, as is often the case, *H* is assumed to be constant, in physical space contours of constant $\sigma << 1$ will conform to the underlying terrain quite closely, while becoming progressively flatter as $\sigma \rightarrow 1$. The downside is that after the transformation, Eq. (2) and the expressions for the velocity components are not as simple as before, but the basic idea remains the same: the vertical velocity is set to whatever value is required to cancel the horizontal divergence. After the field is calculated in (*x, y,* σ)-space, it can be mapped back into (*x, y, z*)-space. Details of this modification can be found in Reynolds, *et al*. (1973). Others who have used Direct-Differencing include Peters & Jouvanis (1979), and Carmichael & Peters (1980).

This category of methods is simple, quick, and straightforward to implement. The problem with such a simplistic approach is that it ignores the observational and interpolative errors that u_i and v_i inevitably contain, and places the entire burden of satisfying Eq. (1) on the vertical component alone. Such a model is clearly inappropriate for stable conditions, where one expects *w* to be of very small magnitude. Even in unstable conditions, unless one starts with very accurate estimates for u_i and v_i, it is quite possible to end up with a *w*-field of unreasonably large magnitude. The resulting winds will not go through obstacles, but they may be biased in favor of going over some that they should be going around. For these reasons, the Direct-Differencing approach appears never to have developed a wide following.

The three papers discussed above apply finite differences to a given (*u,v*) field to get the horizontal divergence, and then compute *w* in such a way as to cancel it. Two additional papers bear mentioning here, those by Anderson (1971) and Liu and Yocke (1980). Rather than compute *w* from a given (*u,v)* field, they compute *u* and *v* by requiring that they just cancel the divergence created by differencing a given *w* field. Though such situations are atypical, at least as far as those scenarios NEST is likely to encounter, they are included here for completeness. The discussion below most closely follows that of Liu and Yocke (1980), who were interested primarily in applying their model to the siting of wind turbines, rather than pollutant migration. They divide their domain into multiple vertical layers, and rewrite Eq. (1) as follows:

$$\frac{\partial \bar{u}_k}{\partial x} + \frac{\partial \bar{v}_k}{\partial y} = -\frac{\partial w}{\partial z} \approx \frac{w(z_{k-1}) - w(z_k)}{\Delta z_k} \tag{4}$$

where $\bar{u}_k$ and $\bar{v}_k$ are averages over the vertical layer extending from z_{k-1} to z_k. It is then assumed that the flow in the horizontal plane is only weakly rotational, *i.e.*,

$$\frac{\partial \bar{v}_k}{\partial x} - \frac{\partial \bar{u}_k}{\partial y} \approx 0 \tag{5}$$

This in turn implies the existence of a 2D scalar potential in each layer, ϕ_k, such that $\bar{u}_k$ and $\bar{v}_k$ can be obtained from its gradient:

$$(\bar{u}_k, \bar{v}_k) \;=\; \nabla_{2D}\phi_k \tag{6}$$

where ∇_{2D} is the 2D horizontal operator $(\partial/\partial x)\hat{i} + (\partial/\partial y)\hat{j}$. When Eq. (6) is substituted into the left-hand side of Eq. (4), the result is

$$\nabla^2_{2D}\phi_k \;=\; \frac{w_i(z_{k-1}) - w_i(z_k)}{\Delta z_k} \tag{7}$$

The given $w_i(z)$ field is differenced to get the right-hand side of Eq. (7), followed by the solution of the Poisson equation for the ϕ_k field (and hence $\bar{u}_k$ and $\bar{v}_k$ from Eq. (6)) needed to just cancel it. The solution of Eq. (7) typically requires an iterative numerical technique. Rather than rely on measurements for $w_i(z)$, Liu and Yocke (1980) parameterize it by relating w at the surface to the terrain slope, and assume that the field decays exponentially with height. Details can be found in their paper.

Much the same idea was applied by Anderson (1971), except that his analysis does not subdivide the domain into multiple vertical layers. Rather, a relation similar to Eq. (4) above is integrated across a single layer extending from the surface at $z = h$ up to the top of the domain, H. This results in a Poisson equation for the scalar potential very similar to Eq. (7), with the right-hand side changed to $\bar{v} \cdot \nabla h$. Such a model can provide layer-averaged horizontal variations in u and v, but no information regarding their vertical profiles.

For NEST-type applications, it is far more likely that (u, v) observations will be available than data on w, so it is doubtful the approach taken by these last two models would be useful in most situations. Yet they have been put to good use as components of larger schemes. For example, the hybrid model developed by Goodin, *et al.* (1980), described in more detail in §2.3, uses a scheme similar to Anderson's (1971) to correct u and v in the surface layer for local terrain effects. And the parameterization of *w(z)* developed by Liu and Yocke (1980) is used in the CALMET model (*cf.* Scire *et al.* (2000), Chapter 2) to adjust for kinematic terrain effects.

Intentionally Left Blank

2.2 Point-Iterative

This approach to satisfying Eq. (1) was begun by Endlich (1967), who first developed the scheme for 2D flow. It is thus applicable only when the vertical component of wind is zero, or in any case contributes negligibly to the divergence. Let the 2D horizontal divergence, δ, and the vertical component of vorticity, ω, be defined by:

$$\frac{\partial u}{\partial x} + \frac{\partial v}{\partial y} = \delta \tag{8}$$

$$\frac{\partial v}{\partial x} - \frac{\partial u}{\partial y} = \omega \tag{9}$$

Endlich's scheme adjusts the horizontal components u and v in such a way that δ is cancelled, while preserving the original ω. If the above equations are discretized about point (i, j)† of the Cartesian grid shown in Fig. 1 below using centered, second-order differences, the result is:

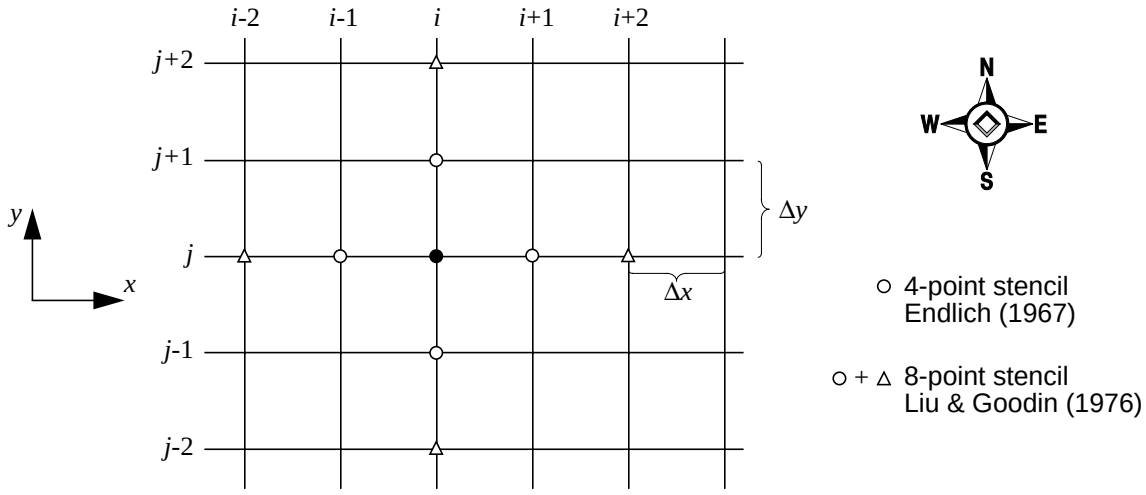

Figure 1. Finite-Difference Stencils Used in Point-Iterative Schemes

$$\frac{u^n_{i+1,\,j} - u^n_{i-1,\,j}}{2\Delta x} + \frac{v^n_{i,\,j+1} - v^n_{i,\,j-1}}{2\Delta y} = \delta^n_{ij} \tag{10}$$

$$\frac{v^n_{i+1,\,j} - v^n_{i-1,\,j}}{2\Delta x} - \frac{u^n_{i,\,j+1} - u^n_{i,\,j-1}}{2\Delta y} = \omega^n_{ij} \tag{11}$$

The superscript n is an index denoting successive iterates in the numerical procedure described below. Thus $n = 0$ corresponds to the initial guess at the (u,v) field, whether it be from interpolated observations or some other source.

†We use i, j indices here to maintain a consistent notation throughout; note that Endlich uses indices k and j, where j and y increase in opposing directions.

At the start of each iteration (or the initial guess), we know u^n and v^n, from which we can evaluate δ^n, which we wish to zero out, and ω^n, which we wish to preserve at its initial value $\omega^n = \omega^o$, from Eqs. (10) and (11). The four-point finite-difference stencil used by these equations is indicated by the open circles, "$\circ$", in Fig. 1. The iterative portion of Endlich's scheme consists of applying the following two steps on a point-by-point basis to go from iterate n to $n+1$:

1. Add corrections of equal magnitude, but opposite sign, to u^n at the points East and West of (i, j); we call these $\pm\bar{u}_{i,j}$. Similarly, corrections $\pm\bar{v}_{i,j}$ of equal magnitude but opposite sign are applied to v^n at the points North and South of (i, j). Substitute these changes into Eq. (10), with the requirement that the divergence vanish as a result:

$$\frac{(u^n_{i+1,j} + \bar{u}_{ij}) - (u^n_{i-1,j} - \bar{u}_{ij})}{2\Delta x} + \frac{(v^n_{i,j+1} + \bar{v}_{ij}) - (v^n_{i,j-1} - \bar{v}_{ij})}{2\Delta y} = 0$$

   If we subtract Eq. (10) from the above equation we are left with simply,

$$\frac{\bar{u}_{ij}}{\Delta x} + \frac{\bar{v}_{ij}}{\Delta y} = -\delta^n_{ij} \tag{12}$$

   Assuming that u and v contribute equally[†] to cancelling δ_{ij}, it follows that

$$\begin{aligned} \bar{u}_{ij} &= -\frac{\Delta x}{2}\delta^n_{ij} \\ \bar{v}_{ij} &= -\frac{\Delta y}{2}\delta^n_{ij} \end{aligned} \tag{13}$$

   We denote the results of this first correction by,

$$\begin{aligned} u^{n+1}_{i\pm1,j} &= u^n_{i\pm1,j} \pm \bar{u}_{ij} \\ v^{n+1}_{i,j\pm1} &= v^n_{i,j\pm1} \pm \bar{v}_{ij} \end{aligned} \tag{14}$$

   Note that while Eq. (14) enforces the condition $\delta_{ij} = 0$, it has absolutely no effect on $\omega_{k,j}$. This follows from the fact that only u at the East/West points and v at the North/South points have been altered, while Eq. (11) depends only on u at the North/South points and v at the East/West points, which remain unchanged.

2. Nevertheless, one must assume that corrections already made on the current iteration to adjust δ and ω at *neighboring* points will have resulted in $\omega^n_{ij} \neq \omega^o_{ij}$. To counter the latter effect, we next add corrections $\pm\hat{u}_{ij}$ of equal magnitude but opposite sign to u^n at the points North and South of (i, j); and similarly, corrections $\pm\hat{v}_{ij}$ of equal magnitude but opposite sign are added to v^n at the East and West points. That is,

[†]Endlich points out that other weightings are possible, but claims that the end results differ very little regardless of what assumption is made as to the relative contribution of u and v. No predictions based on other possible weightings of the two components are shown to support this contention.

$$u^{n+1}_{i,\,j\pm1} = u^{n}_{i,\,j\pm1} \pm \hat{u}_{ij}$$
$$v^{n+1}_{i\pm1,\,j} = v^{n}_{i\pm1,\,j} \pm \hat{v}_{ij} \tag{15}$$

Since, as noted above, the stencils for δ and ω are mutually exclusive, this has no affect on δ_{ij}, which was just zeroed out. With this second correction, and the requirement that ω^{n}_{ij} revert to ω^{o}_{ij}, Eq. (11) now reads:

$$\frac{(v^{n}_{i+1,\,j} + \hat{v}_{ij}) - (v^{n}_{i-1,\,j} - \hat{v}_{ij})}{2\Delta x} - \frac{(u^{n}_{i,\,j+1} + \hat{u}_{ij}) - (u^{n}_{i,\,j-1} - \hat{u}_{ij})}{2\Delta y} = \omega^{o}_{ij}$$

Subtracting Eq. (11) from the above equation leaves,

$$\frac{\hat{v}_{ij}}{\Delta x} + \frac{\hat{u}_{ij}}{\Delta y} = \omega^{o}_{ij} - \omega^{n}_{ij} \tag{16}$$

As before, assuming *u* and *v* contribute equally to correcting ω results in:

$$\hat{u}_{ij} = \frac{\Delta y}{2}(\omega^{o}_{ij} - \omega^{n}_{ij})$$
$$\hat{v}_{ij} = \frac{\Delta x}{2}(\omega^{o}_{ij} - \omega^{n}_{ij}) \tag{17}$$

At this stage, the velocity field given by Eqs. (14) and (15) satisfies both $\delta_{ij} = 0$, and $\omega_{ij} = \omega^{o}_{ij}$ at the point (i, j). The same two-step procedure is then applied at the next point, until the entire domain has been updated. It must be expected that after updating *all* points in the domain for the $(n+1)$st iterate, $\delta_{ij} \neq 0$ and $\omega_{ij} \neq \omega^{o}_{ij}$, at most points anyway, and the *u* and *v* values will be somewhat different from those given by Eqs. (14) and (15). This is the result of the corrections about a given point contaminating those at neighboring points, and is why an iterative process is necessary.

After all points have been updated, *n* is incremented by one, and the process repeated again for the next iteration. Iterations continue until the largest magnitude of δ_{ij} in the domain is less than some (small) predefined number, ε. Endlich (1967) claims that with $\varepsilon = 10^{-6}$ sec^{-1}, convergence is typically achieved within 10-15 iterations. However, it would seem logical to expect the number of iterations required to be a function of both how many grid points the domain contains, and to what extent the original wind field is divergent. Differences in vorticity at the same point between the original and adjusted wind fields are generally of the same order as ε. Endlich himself does not discuss the convergence properties of his iteration scheme, which is analogous to the Gauss-Seidel algorithm often used to solve elliptic equations. However, a companion paper by Stephens (1967) in the same issue of the journal examines its convergence in some detail.

3. After the iterations have converged, one final step remains. The above algorithm can result in an overall increase or decrease in windspeed throughout the domain. To avoid this, the difference between the average over all points of the original and adjusted wind

fields is added to the adjusted wind field at each point. Suppose the above process converges in N iterations; then the final wind field at each point is given by:

$$\begin{aligned} u_{ij} &= u_{ij}^{N} + (\bar{u}^{o} - \bar{u}^{N}) \\ v_{ij} &= v_{ij}^{N} + (\bar{v}^{o} - \bar{v}^{N}) \end{aligned} \qquad \text{for all } i, j \tag{18}$$

where $(\bar{u}^{o}, \bar{v}^{o})$ and $(\bar{u}^{N}, \bar{v}^{N})$ are the average values of the original and iterated wind fields, respectively. This step assures that the average adjusted windspeed is the same as for the original field, and only needs to be performed once. Since the same correction is added to each point, values of δ and ω throughout the field are unaffected.

Because it neglects any contribution from w, such an approach is justified only for stable atmospheric conditions. For such flows, it has the advantage that the flow in each horizontal layer can be treated independent of its neighbors. Also, as noted by Endlich (1967), this approach does not require that boundary conditions be explicitly specified. Rather, the values of u and v at a boundary point are adjusted to cancel δ, and preserve ω, at the neighboring interior point.

Liu and Goodin (1976) claim that the above procedure, while reducing the divergence, nevertheless results in wind fields that differ substantially from the original observations. They suggest a modified scheme that differs from Endlich's in three important respects. First, they introduce a parameter, f_{ij}, which premultiplies the corrections to $\bar{u}_{ij}$ and $\bar{v}_{ij}$ in Eq. (14), and is only allowed to assume a value of zero or one. $f_{ij} = 1$ corresponds to normal field points at which corrections are allowed. However, for grid points at which observational data are available, $f_{ij} = 0$; *i.e.*, no corrections are made at such points, which enforces their requirement that the final field must reproduce the observed data exactly.

Secondly, Liu and Goodin (1976) expand the finite-difference stencil from four to eight points: the original four points used by Endlich, plus four additional points at $(i, j\pm2)$ and $(i\pm2, j)$. The latter are indicated by a " $\triangle$ " in Fig. 1. This introduces three additional artificial parameters: c, η[†] and β. c controls the mixing of information between the original four points and the four new points added to the stencil. If $c = 1$, only the four original " $\circ$ " points are included; $c = 0$ includes only the newer " $\triangle$ " points; intermediate values of c result in a mixture of data from all eight points. η and β are additional factors which premultiply $\bar{u}_{ij}$ and $\bar{v}_{ij}$; η determines what fraction of the velocity corrections is to be applied on each iteration for the original " $\circ$ " points; β serves the same function at the " $\triangle$ " points. Details can be found in the reference.

Lastly, no attempt is made to conserve ω, *i.e.*, Step 2 above in Endlich's original procedure is eliminated. Aside from these three differences, the iteration procedure is carried out point-by-point just as in Endlich's approach. The authors present a brief analysis of the method's convergence, and conclude that the only requirement necessary to assure that the magnitude of δ^n decreases monotonically, and that u^n and v^n converge to definite values, is that $\eta < 1$, independent of β and c. (The latter still have an influence on the final solution, however.)

[†]We've replaced Liu and Goodin's α by η, to avoid confusion with the α factors introduced in §2.4.

While Liu and Goodin's results show the method can reproduce the original observations, they also contain high-frequency components that produce very erratic looking wind-vector plots. The authors claim these are the result of requiring strict reproduction of the observations. They postulate that if this requirement were relaxed by say, allowing the wind at those stations to vary within some prescribed limits about the observed values, the high-frequency components could be removed. However, this introduces yet more *ad hoc* arbitrary parameters into the model. As it is, the authors present no results showing how sensitive the predictions are to the values given to c, η and β, nor do they provide any guidance as to how they should be set beyond the single convergence criterion noted above.

Endlich (1984) later modified his original method in two respects. First, rather than do the calculations in Cartesian space as before, z is transformed to a terrain-following coordinate (TFC), $\sigma = \sigma(z)$. The vertical velocity in the computational (x, y, σ)-space is then neglected. This is tantamount to assuming that the flow remains parallel to lines of constant σ, which by definition are constrained to go over obstacles. So while this model does admit a vertical velocity in physical (x, y, z)-space, it is dictated by purely geometric constraints; atmospheric dynamics are not really the driving force behind w.

The second modification introduced by Endlich (1984) is that, rather than directly differencing values at the grid points as before, here the author differences face-averaged velocities to obtain his corrections. This is more akin to a finite-volume approach, and is likely to be more accurate now that the vertical cell size, $\Delta\sigma$, is a function of x and y. It is asserted that 15-20 iterations are sufficient to reduce the divergence to "small magnitudes" (left unspecified). Whether the method is as computationally efficient as the author claims is left open to question, as no run times are quoted. Predictions based on this updated model are presented for a variety of sites around the United States, but there is a paucity of observations to compare them against. The latter were limited to annual average wind speeds, which is not a very discriminating metric.

Ludwig, *et al.* (1991) sought to generalize Endlich's (1984) procedure by improving on the definition of the σ-coordinate surfaces. The newer approach is termed the Winds On Critical Streamline Surfaces (WOCSS) method, and appeals to the concept of critical dividing streamlines to eliminate the purely geometric construction of the σ-coordinate surfaces. The underlying principle of critical dividing streamlines is that the work that a parcel of fluid must perform against the (buoyant) restoring force in order to just surmount an obstacle can be equated to its original kinetic energy. This allows the derivation of relationships among wind speed, vertical temperature gradient, and the height of an obstacle that the flow can surmount. These relationships allow the definition of a set of quasi-horizontal, two-dimensional surfaces across which no flow occurs, and thus provide a basis for defining coordinate surfaces that, unlike Endlich (1984), incorporates some measure of atmospheric stability. These surfaces will approximate the shape of the flow, but will intersect the terrain in areas where the flow is unable to pass over it.

The flow in each layer defined by two such adjacent surfaces is adjusted independently of the others using Endlich's (1967,1984) two-dimensional Point-Iterative scheme to achieve non-divergence. Winds are set to zero at grid points below the local terrain height; the authors claim that subsequent adjustments to remove the divergence where surfaces intersect the terrain will

cause the flow to pass around the obstacle, rather than being predisposed to go over it, as was the case with Endlich's (1984) analysis. The major weaknesses of the WOCSS method are that it applies only when $d\theta/dz > 0$, *i.e.*, stable flows, and that for certain types of flows, some residual divergence will remain in the wind field, complicating its use for subsequent atmospheric transport and diffusion modeling.

The biggest limitation of the methods in this Point-Iterative category is their two-dimensionality. Since *w* is assumed negligible in Endlich (1967) and Liu and Goodin (1976), the divergence can only be reduced by adjusting the horizontal components, *u* and *v*. This makes them suitable only for stable or stratified conditions. In some sense this approach is the converse of Direct-Differencing (§2.1), which places the burden for satisfying Eq. (1) entirely on *w*. It is interesting to note that Endlich himself temporarily made use of a method, based on the Calculus of Variations, which removes such restrictions (Endlich, *et al.* (1982)), before returning to his Point-Iterative scheme in Endlich (1984). The discussion of the Calculus of Variations approach is deferred until §2.4.

2.3 Hybrid

We've seen that the Direct-Differencing approach (§2.1) requires that any nonvanishing divergence be eliminated by adjusting the vertical velocity, *w*. Models based on this approach are thus not likely to be useful for atmospherically stable conditions, for which the magnitude of *w* is likely to be very small. Conversely, Point-Iterative schemes (§2.2) neglect *w*, and emphasize adjustments to *u* and *v* that will just cancel any horizontal divergence. Such models are inappropriate for convective, or unstable, atmospheric conditions. As its name suggests, the next approach is a hybrid of the first two which attempts to spread responsibility for satisfying Eq. (1) across all three wind components, and hopefully prove reliable under a broader spectrum of conditions.

Goodin *et al.* (1980) were the first to attempt such a combined approach. Their procedure consists of the following steps:

1. An initial surface wind field, u_i and v_i, is obtained from an inverse distance-squared weighted interpolation of available observations, or other appropriate analysis. Gross terrain features, such as mountains, are accounted for by the use of barriers to flow during the interpolation.

2. The following 2D Poisson equation,

$$\nabla^2\phi = \psi(x, y) \tag{19}$$

   is solved using an Alternating-Direction Implicit (ADI) scheme (Peaceman and Rachford (1955)). Here ϕ is a velocity potential, and ψ is a forcing function that is said to depend on the domain thickness and terrain gradients. The resulting irrotational velocity field is used to adjust the previously interpolated surface field for local terrain effects. Unfortunately, the authors are vague as to just how ψ is specified, or how the irrotational velocity, $\nabla\phi$, is combined with the interpolated field, saying only that they used a technique "similar to that of Anderson (1971)".

3. Thus far only the horizontal surface winds have been defined. Due to the relative scarcity and imprecision of vertical profile observations, *u* and *v* at elevations above the surface are interpolated using a r^{-1}-weighted interpolation scheme. This also provides smoother results than would a r^{-2}-weighted scheme.

4. In principle, one could at this point obtain values for the vertical component everywhere in the domain by applying the Direct-Differencing method described in §2.1. However, as noted there and by Goodin, *et al.* (1980), this is likely to yield unrealistically large values of *w*. Instead, an effort is first made to reduce the divergence in the (*u*, *v*) field by applying the following five-point filter,

$$u_{ij}^{n+1} = \gamma_{ij} u_{ij}^{n} + (1 - \gamma_{ij}) \left(\frac{u_{ij}^{n} + u_{i+1,\,j}^{n} + u_{i-1,\,j}^{n} + u_{i,\,j+1}^{n} + u_{i,\,j-1}^{n}}{5} \right) \tag{20}$$

   which sets the new value of *u* equal to a weighted average of the old value at the same point, and that of its nearest four neighbors; the same formula is used for *v* as well. It is

applied on a point-by-point basis throughout each horizontal layer, except for the bottom-most layer next to the ground. The subscripts *i* and *j* are integer indices along *x* and *y*, respectively, and the superscript *n* denotes the number of sweeps taken. γ_{ij} is a user-prescribed weighting factor that in principle can vary from point to point. $\gamma_{ij} = 1$ can be set at grid points at or very near observation stations to preserve those data, with $\gamma_{ij} = 0$ at other points, giving their values free rein to adjust as needed. Values between these extremes can be used to specify some mixture of adherence to the original data *vs*. adjusted values.

Though no formal analysis of the filter's effects is given, it is clear that the averaging process has the effect of smoothing the field at all points with $\gamma_{ij} < 1$. As the number of sweeps is increased, the field will become progressively more uniform and less divergent. This number may vary from one vertical layer of the grid to another. The authors suggest that the appropriate amount of smoothing can only be determined empirically. They state that "This step is designed to reduce as much of the *anomalous* divergence as possible… A relatively unstable (generally near ground level) layer requires few iterations since less of the divergence present is *anomalous*, while a more stable upper layer must be smoothed more times." Anomalous as contrasted to what? According to Eq. (1), *all* of the divergence is anomalous. Note that this step adjusts only the horizontal wind components.

5. A terrain-following coordinate (again renamed σ here) is introduced. The authors never give an explicit definition for $\sigma(z)$, but note that it varies from 0 at the surface to 1 at the top of the domain, which is consistent with the definition given here by Eq. (3) in §2.1. The continuity equation, when transformed to the TFC system (x, y, σ), and setting the divergence to zero, reads:

$$\frac{\partial W}{\partial \sigma} = -\left[\frac{\partial (u\Delta H)}{\partial x} + \frac{\partial (v\Delta H)}{\partial y}\right] \tag{21}$$

where $\Delta H = H(x,y,t) - h(x,y)$[†], and W is the vertical velocity in the TFC system, related to that in Cartesian coordinates, w, by,

$$W = w - u\left(\frac{\partial h}{\partial x} + \sigma\frac{\partial \Delta H}{\partial x}\right) - v\left(\frac{\partial h}{\partial y} + \sigma\frac{\partial \Delta H}{\partial y}\right) - \sigma\frac{\partial \Delta H}{\partial t} \tag{22}$$

Equation (21) is integrated for $W(\sigma)$ layer by layer, starting from $\sigma = 0$, using the (u, v) field from Step 4. This is very much like the Direct-Differencing approach described in §2.1, with one important exception. The result of integrating Eq. (21) across a single vertical layer in the grid extending from *k-1/2* to *k+1/2* can be written,

$$W_{i,\,j,\,k+1/2} = \cancel{0} + W_{i,\,j,\,k-1/2} - (\Delta\sigma)_{ijk}\left[\frac{\partial (u\Delta H)}{\partial x} + \frac{\partial (v\Delta H)}{\partial y}\right]_{ijk} \tag{23}$$

[†]At this point both $H(x,y,t)$ and $h(x,y)$ are assumed to be known functions.

$W_{i,\,j,\,k-1/2}$ represents the vertical velocity at the top of the next lowest layer, which is the bottom of the current layer. In general, it will be nonzero, but Goodin, *et al.* (1980) make the *ad hoc* assumption that $W_{i,\,j,\,k-1/2} = 0$ *for the purposes of this equation only.* The resulting $W_{i,\,j,\,k+1/2}$ is in turn neglected for the purposes of calculating $W_{i,\,j,\,k+3/2}$, and so on. The authors reason that doing so prevents the accumulation of errors in *W*, thus avoiding unrealistically large values near the top of the domain. The evaluation of Eq. (23) in each layer is thus completely decoupled from that in adjacent layers. This step results in altering only *W*, and—through Eq. (22)— the *w* component of wind velocity in physical space. The generally nonzero *W* values that result are used in the next step, during which they are frozen at the current values.

6. The wind field must still be expected to retain some divergence. At this point the authors specialize the analysis to the case $\Delta H = H(x,y,t) - h(x,y) \approx$ constant. In this case Eq. (21), with nonzero 3D divergence D_{ijk} at grid point (i,j,k) can be approximated using centered finite differences as,

$$D^n_{ijk} = \Delta H\left[\frac{u^n_{i+1/2,\,j,\,k} - u^n_{i-1/2,\,j,\,k}}{\Delta x} + \frac{v^n_{i,\,j+1/2,\,k} - v^n_{i,\,j-1/2,\,k}}{\Delta y}\right] + \frac{W_{i,\,j,\,k+1/2} - W_{i,\,j,\,k-1/2}}{\Delta\sigma} \tag{24}$$

where the superscript *n* is again an iteration counter; the terms involving *W* do not contain it, since, as noted above, *W* is considered frozen during this step. In the same spirit as the Point-Iterative approach of §2.2, we imagine corrections of equal magnitude, but opposite sign, applied to *u* at the points just east and west of (i,j,k), and to *v* at the points just to the north and south, as follows:

$$\begin{aligned} u^{n+1}_{i\pm1/2,\,j,\,k} &= u^n_{i\pm1/2,\,j,\,k} \pm \bar{u}_{ijk} \\ v^{n+1}_{i,\,j\pm1/2,\,k} &= v^n_{i,\,j\pm1/2,\,k} \pm \bar{v}_{ijk} \end{aligned} \tag{25}$$

Equation (24) evaluated at the next iterate would read, with $D^{n+1}_{ijk} = 0$,

$$0 = \Delta H\left[\frac{u^{n+1}_{i+1/2,\,j,\,k} - u^{n+1}_{i-1/2,\,j,\,k}}{\Delta x} + \frac{v^{n+1}_{i,\,j+1/2,\,k} - v^{n+1}_{i,\,j-1/2,\,k}}{\Delta y}\right] + \frac{W_{i,\,j,\,k+1/2} - W_{i,\,j,\,k-1/2}}{\Delta\sigma} \tag{26}$$

The values $\bar{u}_{ijk}$ and $\bar{v}_{ijk}$ need to take on in order to just cancel D^n_{ijk} can be determined by subtracting Eq. (24) from Eq. (26), and then substituting from Eq. (25). The result is

$$-D^n_{ijk} = \Delta H\left[\frac{2\bar{u}_{ijk}}{\Delta x} + \frac{2\bar{v}_{ijk}}{\Delta y}\right]$$

Assuming that, on average, both terms on the right contribute equally to cancelling the divergence, we have,[†]

$$\bar{u}_{ijk} = -\frac{\Delta x}{4\Delta H} D^n_{ijk} \qquad \bar{v}_{ijk} = -\frac{\Delta y}{4\Delta H} D^n_{ijk} \tag{27}$$

No attempt is made to preserve the vertical component of vorticity. While Eqs. (25) and (27) together cancel the remaining divergence at (i,j,k), they can be expected to contaminate the divergence at neighboring points. This is why an iterative process is again needed. The above corrections are applied on a point-by-point basis in each horizontal layer to complete one iteration, and then the field is swept again. The number of iterations required no doubt depends on the magnitude of the divergence field at the start, and how low one wishes to drive it. On the latter point, Goodin, *et al.* (1980) say only that "the magnitude of the divergence should be less than the local vertical velocity and less than the estimated errors in the horizontal velocity components." Given that divergence and velocity have different units, such direct numerical comparisons would be inappropriate, leaving this criterion open to some interpretation.

Goodin, *et al.* (1980) used the above procedure to model the air flow over the Los Angeles area using a 100×50 horizontal grid with $\Delta x = \Delta y = 3.2$ km, and 5 vertical layers of varying depth. The algorithm is said to have reduced the divergence to less than 0.001 sec^{-1} in all the layers, which took ~ 5 min of CPU time on an IBM 370 computer. It is difficult to assess how much of a reduction this represents without knowing the magnitude of the original divergence field, which is not given. However, if one were to simply assign random numerical values of O(1 m/sec)—based on their Figs. 1, 4b, and 9— to u and v over a 3.2 km grid spacing, the magnitude of the resulting divergence would be no worse than ~ $O(10^{-3}$–10^{-2} $\text{sec}^{-1})$. It would appear then that the divergence field was reduced in magnitude by one, or perhaps two, orders of magnitude. It will be seen later that this is much less of a reduction than can be obtained using the Variational Calculus approach (*cf.* §2.4 here, and also Goodin, *et al.*'s Table 3). Moreover, Table 2 in Goodin, *et al.* (1980) shows that most of their reduction is obtained as a result of the smoothing procedure (Step 4 above), which doesn't make use of Eq. (1).

Pepper, *et al.* (1998) used the above scheme to help set initial conditions for more refined prognostic simulations employing finite elements. Chen, *et al.* (1999) successfully used it to provide meteorological inputs for predicting the transport of a power plant plume over Grand Canyon National Park.

Though the details differ considerably, the DIMCOR diagnostic model (Giarola, *et al.* (1995)) is based on a procedure similar in philosophy to that of Goodin *et al.* (1980) in that it represents a combination of the Direct-Differencing and Point-Iterative schemes applied in succession. Notably, an SST representation of the topography is used instead of Goodin *et al.*'s use of a TFC mapping. The authors present results for adjusted winds over sections of Antarctica using a $44 \times 38 \times 7$ grid. Run times are reported to be ~ 5 min on a 386 PC with math coprocessor running DOS.

[†]This next result is a slight generalization of Goodin, *et al.*'s (1980) Eq. (10) to the case $\Delta x \neq \Delta y$.

The CALMET model (Scire, *et al.* (2000)) also employs a hybrid scheme similar to that described above. It is designed to provide meteorological inputs to the CALPUFF pollutant dispersal model. The original development of both CALMET and CALPUFF was sponsored by the California Air Resources Board for use in a regulatory environment, and they have received extensive use in that state as well as others. The CALMET/CALPUFF suite of codes was formally proposed by the U.S. Environmental Protection Agency (EPA) for inclusion in Appendix A of its *Guideline on Air Quality Models* as a preferred ("Guideline") model for certain types of applications. (See **`http://src.com/calpuff/calpuff1.htm`** and the U.S. EPA SCRAM web site, **`http://www.epa.gov/scram001`**, for details.) Terrain effects are incorporated using a TFC system, as are both overland and overwater boundary layer modules. CALMET has also been modified to make use of satellite cloud data and precipitation data. In addition to accepting observational data as input, interfaces have been developed to accept input winds from the predicted output of the prognostic models MM4 and MM5 (Grell, *et al.* (1994)). Examples of studies that have employed CALMET include those by Godfrey and Clarkson (1998), and Barna, *et al*. (2000a,b).

Another such hybrid model is incorporated as part of the TAMOS emergency response suite of computer codes (Pechinger, *et al.* (2001)). It incorporates a diagnostic model variously described as an "adjustment" of the CALMET model (Pechinger, *et al*. (2001)), and an "improvement" to it (Stohl, *et al.* (1997)). According to Stohl, *et al.* a "first-guess" wind field is modified by parameterization of topographic effects, slope winds, and blocking. Then measured wind data are interpolated to the grid, and a weighted average of these modified first-guess and interpolated wind fields is computed. Finally, Goodin, *et al.*'s (1980) procedure described above is applied to the resulting wind field to reduce the divergence to acceptable levels.

Hybrid procedures such as these represent a patchwork of disparate approaches, each designed to in some way compensate for the deficiencies in the others. But the whole suffers from too many *ad hoc* assumptions and approximations, not to mention lapses in specificity. Notable among these are: the ambiguity in Goodin, *et al.*'s (1980) description of Step 2—"similar to that of Anderson (1971)" leaves room for considerable interpretation; moreover, a careful reading of Anderson (1971) reveals that it is a small-perturbation analysis linearized about a mean flow, valid only for very small slopes, and hence inapplicable to mountainous terrain; the splitting of Steps 5 (Direct-Differencing to get w) and 6 (Point-Iterative divergence-reduction by adjustment of u, v), when in fact the physics does the two simultaneously; the neglect of $W_{i,\,j,\,k-1/2}$ in Eq. (23); and the assumption that u and v each contribute equally to reducing the divergence at every point. There are also several user-specified parameters whose values can only be known empirically, *i.e.*, with the benefit of 20/20 hindsight. Among the latter are the appropriate values of γ_{ij} for use in Eq. (20), the number of smoothing iterations to perform (Step 4), and the number of iterations to apply to Point-Iterative divergence-reduction (Step 6). Indeed, the magnitude of w relative to u and v is likely to depend in large measure on the number of iterations spent in Step 4 *vs.* Step 6. As Goodin, *et al.* point out, this will likely depend on the stability properties of the atmosphere at the time, but an objective parameterization of these quantities has yet to be developed. Hence there remains a good deal of subjectivity in applying this approach to new terrain for which the model has yet to be "tuned".

Intentionally Left Blank

2.4 Variational Calculus

The groundwork for the application of the calculus of variations to this problem was laid in the paper by Sasaki (1958), and later updated and extended by him in Sasaki (1970a,b). Though he considered some simple examples to illustrate the method, it wasn't until the late 1970s that the formalism was embodied in practical computer programs that automated the process. The first appears to have been MASCON, a two-dimensional flux model developed by Dickerson (1978) at the Lawrence Livermore National Laboratory to supply meteorological inputs to air pollution models of the San Francisco Bay area. This was soon followed by MATHEW (Sherman, (1978)), which extended the variational formalism to three dimensions, and provided inputs to the ADPIC pollutant transport model (Lange, (1978)). The development below most closely parallels that of Sherman (1978), and fills in some details that have been glossed over in the literature.

The calculus of variations deals with the concept of a *functional*, as contrasted with the more traditional *function*. The value of a given *function*, say $f(x)$, is known once the value of the independent variable x is specified. A *functional*, on the other hand, is itself defined in terms of one or more arbitrary functions, such that its value is known only after each such function has been given a specific form. For present purposes, the particular functional of interest is the following volume integral (*cf.* Sherman (1978), Eq. (1)):

$$E(u, v, w, \lambda) = \int_V \Big[\alpha_1^2 (u - u_i)^2 + \alpha_1^2 (v - v_i)^2 + \alpha_2^2 (w - w_i)^2 + \lambda \left(\frac{\partial u}{\partial x} + \frac{\partial v}{\partial y} + \frac{\partial w}{\partial z} \right) \Big] dx\,dy\,dz \tag{28}$$

E is a *functional* because its value depends on the specific form of the *functions* u, v, w, and λ that appear in the integrand. The integral is over the entire computational volume. u_i, v_i, and w_i denote the components of the observed (interpolated) wind field with which the calculation is begun; these are fixed quantities. On the other hand, u, v, and w represent the adjusted wind field for which we will be solving; each in turn is a function of x, y, and z. α_1 and α_2 are termed "Gauss precision moduli." More will be said about them in due course; for now they may be thought of as weighting factors which are presumed to be specified *a priori*. Finally, $\lambda(x,y,z)$ is the so-called Lagrange multiplier, which is also to be determined as part of the solution. The terms on the first line represent a weighted mean-square deviation between the adjusted and initial wind fields; the factor in parentheses on the second line is the divergence we seek to eliminate. The variational approach seeks those functions u, v, w and λ such that the integral of the two terms over the domain is as small as possible—*i.e.*, we seek to minimize E. This formulation is the one referred to by Sasaki as being subject to a "strong constraint" (Sasaki (1970a), §3). The reader desiring a more in-depth discussion of the calculus of variations itself is referred to the texts by Weinstock (1952), Courant and Hilbert (1953), and Schecter (1967).

In principle, each wind component could be assigned a different weighting factor, for a total of three. But as noted by Sherman (1978), assigning different weights to each of u and v would seem specious, so both are premultiplied by the same α_1. (This point is raised again later, on p. 35.) Originally, the magnitudes of α_1 and α_2 were related to the confidence level in their respective components' observed values; *i.e.*, $\alpha^2 = (1/2)\sigma^{-2}$, where σ^2 is the presumed variance

of the error in the corresponding field. Thus, a large value for α_1^2 (α_2^2) constrains the adjusted field of the horizontal (vertical) components to remain close to the initial field in Eq. (28); conversely, a small weighting factor allows larger deviations between the two.

Just as $f'(x_m) = 0$ is necessary for $f(x_m)$ to be a minimum of the function f, a necessary condition for the minimization of the functional E is that its first variation, δE, vanish (*cf*. the texts cited above). It can be shown that: a) most of the rules for differentiation, *e.g.*, the chain rule, apply also to taking variations; and b) the variational operator δ commutes with the processes of differentiation and integration. Therefore, taking the first variation of Eq. (28) and setting it to zero yields,

$$\delta E = \int_V \Big[2\alpha_1^2(u-u_i)\delta u + 2\alpha_1^2(v-v_i)\delta v + 2\alpha_2^2(w-w_i)\delta w + \lambda\left(\frac{\partial(\delta u)}{\partial x} + \frac{\partial(\delta v)}{\partial y} + \frac{\partial(\delta w)}{\partial z}\right) + \left(\frac{\partial u}{\partial x} + \frac{\partial v}{\partial y} + \frac{\partial w}{\partial z}\right)\delta\lambda \Big] dxdydz = 0 \qquad (29)$$

Note that all the terms are linearly proportional to either δu, δv, δw, or $\delta\lambda$, *except* the middle term proportional to λ, which involves derivatives such as $\partial(\delta u)/\partial x$, *etc*. For reasons that will become clear below, these terms need to be put in a form such that they too are linearly proportional to just the variations and not their derivatives. For the moment consider just the portion of the term in question that involves $\partial(\delta u)/\partial x$,

$$\int_V \lambda\frac{\partial(\delta u)}{\partial x}dxdydz = \int_{z_1}^{z_2}dz\int_{y_1}^{y_2}dy\int_{x_1}^{x_2}\lambda\frac{\partial(\delta u)}{\partial x}dx = \int_{z_1}^{z_2}dz\int_{y_1}^{y_2}dy\left[(\lambda\delta u)\Big|_{x_1}^{x_2} - \int_{x_1}^{x_2}\delta u\frac{\partial\lambda}{\partial x}dx\right]$$

where x_1, x_2, *etc*., represent the bounding planes of the rectangular computational domain, and the second equality follows from an integration-by-parts with respect to x. It should be clear that the other portions of the term, those involving derivatives of δv and δw, can be handled in like manner if the integration-by-parts is done with respect to y and z, respectively. This transforms Eq. (29) to:

$$\delta E = \int_{z_1}^{z_2}\int_{y_1}^{y_2}\int_{x_1}^{x_2}\Big[2\alpha_1^2(u-u_i)\delta u + 2\alpha_1^2(v-v_i)\delta v + 2\alpha_2^2(w-w_i)\delta w - \left(\delta u\frac{\partial\lambda}{\partial x} + \delta v\frac{\partial\lambda}{\partial y} + \delta w\frac{\partial\lambda}{\partial z}\right) + \left(\frac{\partial u}{\partial x} + \frac{\partial v}{\partial y} + \frac{\partial w}{\partial z}\right)\delta\lambda \Big] dxdydz \qquad (30)$$

$$+ \int_{z_1}^{z_2}\int_{y_1}^{y_2}\Big[(\lambda\delta u)\Big|_{x_1}^{x_2}\Big]dydz + \int_{z_1}^{z_2}\int_{x_1}^{x_2}\Big[(\lambda\delta v)\Big|_{y_1}^{y_2}\Big]dxdz + \int_{y_1}^{y_2}\int_{x_1}^{x_2}\Big[(\lambda\delta w)\Big|_{z_1}^{z_2}\Big]dxdy = 0$$

Next collect terms proportional to δu, δv, δw, and $\delta\lambda$,

$$\delta E = \int_V \left\{ \left[2\alpha_1^2 (u - u_i) - \frac{\partial \lambda}{\partial x} \right] \delta u + \left[2\alpha_1^2 (v - v_i) - \frac{\partial \lambda}{\partial y} \right] \delta v + \left[2\alpha_2^2 (w - w_i) - \frac{\partial \lambda}{\partial z} \right] \delta w \right.$$
$$\left. + \left(\frac{\partial u}{\partial x} + \frac{\partial v}{\partial y} + \frac{\partial w}{\partial z} \right) \delta\lambda \right\} dx dy dz \qquad (31)$$
$$+ \int_{z_1}^{z_2} \int_{y_1}^{y_2} \left[(\lambda \delta u) \Big|_{x_1}^{x_2} \right] dy dz + \int_{z_1}^{z_2} \int_{x_1}^{x_2} \left[(\lambda \delta v) \Big|_{y_1}^{y_2} \right] dx dz + \int_{y_1}^{y_2} \int_{x_1}^{x_2} \left[(\lambda \delta w) \Big|_{z_1}^{z_2} \right] dx dy = 0$$

Assume for the moment that the terms evaluated on the domain boundaries, *i.e.*, those in the last line of Eq. (31), all vanish (we will return to this point later). The remaining integrand consists of terms which are each proportional to one of δu, δv, δw, or $\delta\lambda$. For Eq. (31) to be satisfied for *arbitrary* variations δu, δv, δw, and $\delta\lambda$, the coefficients multiplying each of these quantities must themselves be zero *at every point of the domain, i.e.*,

$$2\alpha_1^2 (u - u_i) - \frac{\partial \lambda}{\partial x} = 0 \qquad \Rightarrow \qquad u = u_i + \frac{1}{2\alpha_1^2} \frac{\partial \lambda}{\partial x} \qquad (32a)$$

$$2\alpha_1^2 (v - v_i) - \frac{\partial \lambda}{\partial y} = 0 \qquad \Rightarrow \qquad v = v_i + \frac{1}{2\alpha_1^2} \frac{\partial \lambda}{\partial y} \qquad (32b)$$

$$2\alpha_2^2 (w - w_i) - \frac{\partial \lambda}{\partial z} = 0 \qquad \Rightarrow \qquad w = w_i + \frac{1}{2\alpha_2^2} \frac{\partial \lambda}{\partial z} \qquad (32c)$$

$$\frac{\partial u}{\partial x} + \frac{\partial v}{\partial y} + \frac{\partial w}{\partial z} = 0 \qquad (32d)$$

At first glance, this might appear sufficient, but perhaps not necessary. To see why this is in fact both necessary and sufficient, consider the consequences if Eqs. (32a)-(32d) are *not* satisfied at every point of the domain. That would imply the coefficients of δu, δv… could be either positive or negative over some finite portion of the volume. By choosing δu, δv… such that each always had the same sign as its coefficient, we could force the integrand to always be positive, thus causing $\delta E > 0$, in violation of Eq. (31). To repeat, the only way to enforce $\delta E = 0$ for any and all variations δu, δv… is to satisfy Eqs. (32a)-(32d) at every point. The first three of these equations show that the adjusted wind field at each point equals the initial field plus correction terms that are suitably-weighted derivatives of the Lagrange multiplier. The last equation is simply Eq. (1) written in Cartesian coordinates. Equations (32a)–(32d) agree with Sherman's (1978) Eqs. (2)–(5).

The above system consists of four partial differential equations (PDEs) in the four unknowns, u, v, w, and λ. However, the first three of these can be eliminated by substituting Eqs. (32a)–(32c) into Eq. (32d), resulting in a single PDE for λ:

$$\frac{\partial u_i}{\partial x} + \frac{\partial}{\partial x}\left(\frac{1}{2\alpha_1^2}\frac{\partial \lambda}{\partial x}\right) + \frac{\partial v_i}{\partial y} + \frac{\partial}{\partial y}\left(\frac{1}{2\alpha_1^2}\frac{\partial \lambda}{\partial y}\right) + \frac{\partial w_i}{\partial z} + \frac{\partial}{\partial z}\left(\frac{1}{2\alpha_2^2}\frac{\partial \lambda}{\partial z}\right) = 0$$

or rearranging,

$$\frac{\partial}{\partial x}\left(\frac{1}{2\alpha_1^2}\frac{\partial \lambda}{\partial x}\right) + \frac{\partial}{\partial y}\left(\frac{1}{2\alpha_1^2}\frac{\partial \lambda}{\partial y}\right) + \frac{\partial}{\partial z}\left(\frac{1}{2\alpha_2^2}\frac{\partial \lambda}{\partial z}\right) = -\left(\frac{\partial u_i}{\partial x} + \frac{\partial v_i}{\partial y} + \frac{\partial w_i}{\partial z}\right) \tag{33}$$

This result is valid for the general case where α_1 and α_2 are allowed to vary with position in the field. In practice, they are typically assumed to be constants, in which case the result can be written,

$$\frac{\partial^2 \lambda}{\partial x^2} + \frac{\partial^2 \lambda}{\partial y^2} + \left(\frac{\alpha_1^2}{\alpha_2^2}\right)\frac{\partial^2 \lambda}{\partial z^2} = -2\alpha_1^2\left(\frac{\partial u_i}{\partial x} + \frac{\partial v_i}{\partial y} + \frac{\partial w_i}{\partial z}\right) \tag{34}$$

This is Sherman's (1978) Eq. (9). The parenthetical expression on the right-hand side is the divergence field of the initial wind, which is known. Thus Eq. (34) represents an elliptic Poisson-like PDE for the unknown λ.

However, obtaining a unique solution also requires that boundary conditions on λ be specified. Recall that on p. 23 it was assumed, without justification, that all the terms on the last line in Eq. (31) vanished. Sufficient conditions for this to be the case are:

$$\lambda \delta u = 0 \qquad \text{on } x_1, x_2 \tag{35a}$$

$$\lambda \delta v = 0 \qquad \text{on } y_1, y_2 \tag{35b}$$

$$\lambda \delta w = 0 \qquad \text{on } z_1, z_2 \tag{35c}$$

that is, the product of λ times the variation in velocity normal to each boundary must vanish. These are the same conditions stated by Sherman (1978) as her Eqs. (6)–(8). As noted by Sherman, they can be used to simulate a variety of boundary types, as follows.

Specifying $\lambda = 0$ at a boundary clearly satisfies Equations (35a)–(35c). In general its nearest interior neighbor in the solution will have a nonzero value; *i.e.*, the gradient of λ normal to the boundary, $\partial\lambda/\partial n$, will be nonzero. Equations (32a)–(32c) indicate that the normal velocity across the boundary will vary accordingly, implying that the amount of fluid crossing the boundary will adjust to the interior solution. Thus, setting $\lambda = 0$ is appropriate for throughflow boundaries of indeterminate flux, as would typically be the case on the lateral faces (at x_1, x_2, y_1, y_2) of the computational domain. Further, since $\lambda = 0$ across the entire boundary, the gradients in the plane of the boundary are also zero, meaning that the two transverse components of velocity will retain their initial values. This is the situation depicted graphically in Fig. 2(a).

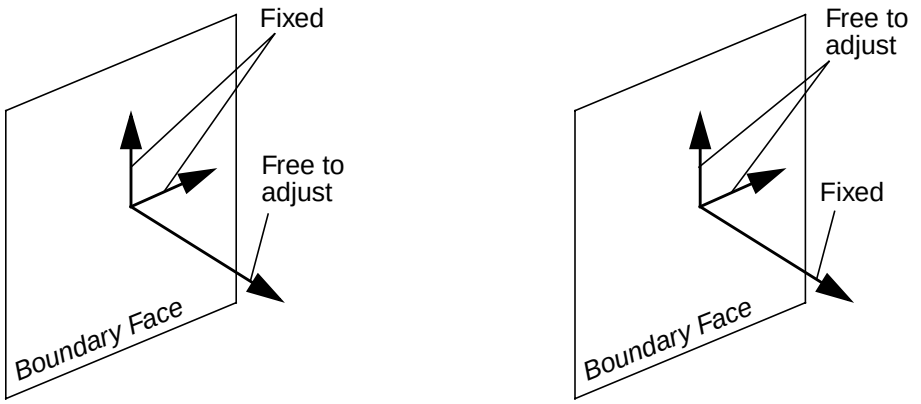

(a) $\lambda = 0$: Throughflow Boundary of Unknown Flux

(b) $\partial\lambda/\partial n = 0$: Throughflow Boundary of Known Flux

Figure 2. Choice of Boundary Conditions for λ

Alternatively, one could set the gradient of λ normal to a bounding surface to zero; that is, $\partial\lambda/\partial n = \partial\lambda/\partial(x,y,z) = 0$, as appropriate. Equations (32a)–(32c) tell us this is tantamount to requiring that the normal velocity there remain unchanged from its initial value, *i.e.*, δu (or δv, or δw, as appropriate) = 0 there, which is another way of satisfying Eqs. (35a)–(35c). Hence $\partial\lambda/\partial(x,y,z) = 0$ is appropriate for use at throughflow boundaries with a known flux, as specified by a nonzero normal velocity in the initial field. This is also the appropriate condition to use at an impermeable boundary, which is the special case of zero normal initial velocity; this pertains along the bottom boundary of the computational domain. With this boundary condition, the gradients of λ in the plane of the boundary are free to change, thus allowing the two in-plane components of velocity to adjust as necessary. This is the situation shown in Fig. 2(b).

Equation (33) (or (34)) can be solved, subject to a suitable combination of the boundary conditions just described, using standard numerical methods, typically based on finite-difference approximations. The resulting λ field is then substituted into Eqs. (32a)-(32c) to obtain the adjusted wind field, (u,v,w), that satisfies Eq. (32d). Barnard, *et al.* (1987), Ross, *et al.* (1988), and Ratto, *et al.* (1994) have all raised an important point that bears repeating: while the procedure just described enforces mass conservation, in and of itself it does nothing to assure that the surface boundary condition is satisfied, as neither Eq. (28) nor Eqs. (32a)-(32d) contain any explicit knowledge of the underlying terrain. The surface winds in the interpolated field must have already been aligned parallel to the topography *before* the above adjustments are made. Use of the impermeable boundary condition in the previous paragraph will then assure that the wind component normal to the surface remains zero.

The Variational Calculus approach has the advantage of treating all three wind components simultaneously in a unified framework, as opposed to forcing any divergence to be cancelled by just one or two components (Direct-Differencing, Point-Iteration), or some *ad hoc* combination of all three (Hybrid). It has also enjoyed more widespread application than the other approaches, as can be seen from Table 1 on p. 4. That is not to say that the present formalism is without ambiguity, the most notable feature in this regard being the two weighting factors, α_1 and α_2.

In this regard it has often been stated in the literature, without elaboration, that the solution of the system represented by Eq. (34) and Eqs. (32a)-(32c) depends only on the ratio α_1/α_2, and not on α_1 and α_2 separately (see, *e.g.*, Ross, *et al.* (1988), and Finardi, *et al.* (1993)). At first glance this would not appear to be the case, since there is no algebraic manipulation that can be applied to these equations to render their coefficients functions of only α_1/α_2. However, consider the following thought experiment. Imagine that we have a solution (u,v,w,λ) for a given interpolated field and suitably chosen values of α_1 and α_2. Now consider the same system with the values of α_1 and α_2 each multiplied by a constant, say c, such that their ratio remains the same. The right-hand side of Eq. (34) will increase by c^2, and since the left-hand side is unchanged the new solution, say λ', will be everywhere increased by the same amount relative to the original, $\lambda' = c^2\lambda$. However, when λ' is substituted into Eqs. (32a)-(32c), the original (u,v,w) will still be recovered. So while the solution for λ does indeed depend on α_1 and α_2 separately, λ is just an artifice we introduced. The only solution of real interest is for the wind field, and that is indeed a function of only a single parameter, α_1/α_2, which is often denoted in the literature by the shorthand α. (Further support for this argument can be found on p. 29 in connection with the COMPLEX model.) Thus, when constant weighting factors are used, it is common to replace the above system with one in which for convenience $\alpha_1 = 1$, and $\alpha_1/\alpha_2 = \alpha$ (Ross, *et al.* (1988), Bradley, *et al.* (1997)):

$$u = u_i + \frac{1}{2}\frac{\partial\lambda}{\partial x} \tag{36a}$$

$$v = v_i + \frac{1}{2}\frac{\partial\lambda}{\partial y} \tag{36b}$$

$$w = w_i + \frac{\alpha^2}{2}\frac{\partial\lambda}{\partial z} \tag{36c}$$

$$\frac{\partial^2\lambda}{\partial x^2} + \frac{\partial^2\lambda}{\partial y^2} + \alpha^2\,\frac{\partial^2\lambda}{\partial z^2} = -2\left(\frac{\partial u_i}{\partial x} + \frac{\partial v_i}{\partial y} + \frac{\partial w_i}{\partial z}\right) \tag{37}$$

From this point on, unless stated otherwise, the discussion will implicitly assume that the weighting factors are constant, so that we can focus on choosing the single parameter α. In the more general case where α_1 and α_2 both vary with position, but in such a way that their ratio remains constant, the above argument for (u,v,w) depending only on α can still be made by replacing Eq. (34) with Eq. (33). However, there seems to be no getting around having to solve the original system, Eqs. (33) and (32a)-(32c), under these assumptions.

Although α_1 and α_2 started out being related to the uncertainty in the observed values on which the interpolated wind field is based, they have evolved over the years into a means of incorporating the degree of atmospheric stability, or lack thereof, into the calculations. In the discussion below of the various models based on this formalism an attempt is made to highlight the differences in how various investigators have chosen values for these weighting factors.

As noted earlier, Sherman (1978) was the first to apply this approach in three dimensions, as embodied in the MATHEW model (*cf.* Table 1). The computational domain consisted of a

rectangular box in (x, y, z), whose bottom coincided with the lowest elevation of interest. A Cartesian grid with uniform Δx, Δy, and Δz was superimposed on the domain. The local surface terrain elevation was modeled by blocking off columns of cells within the rectangular volume such that no flow is allowed in or out of them. This leads to a crude "stair-step terrain" representation of the topography; models employing this technique are indicated in Table 1 with the acronym SST. Its use limits the accuracy to which boundary conditions can be imposed at the surface, and also prevents the use of variable cell depth in the vertical coordinate. The finite-difference approximation to Eq. (34) leads to a system of linear equations whose coefficient matrix is asymmetric and diagonally dominant; Sherman solved it using a numerical method known as Successive Over-Relaxation (SOR) (Forsythe and Wasow (1960)).

Numerical experiments with MATHEW revealed that, as expected, the solutions were strongly influenced by the choice of $\alpha = \alpha_1/\alpha_2$. It was concluded that this ratio should be proportional to the expected magnitude of $(w/u)^2$, or $\alpha^2 \sim 10^{-4}$ for conditions approximating neutral stability. Larger values will result in most of the adjustment being made in w, as would be appropriate for unstable (convective) flows; for smaller values, adjustments to u and v will dominate, as would befit more stable flows. Reductions in the overall divergence magnitude (comparing the interpolated and final adjusted wind fields) by some twelve orders of magnitude were demonstrated. For grids containing 3×10^4 points, run times were on the order of a few minutes on a CDC 7600 machine. MATHEW continues to be actively used by the Atmospheric Release Advisory Capability (ARAC) group at Lawrence Livermore National Laboratory (Sullivan, *et al.* (1993)). Other investigations that have successfully used it have been published by Finardi, *et al.* (1993), Banta, *et al.* (1996), and Givati, *et al*. (1996).

The NOABL model (Traci, *et al.* (1978)) is included in the present category even though it purports not to be based on variational calculus, but on a more intuitive, quasi-potential approach. The authors argue that the air can be viewed as inviscid, which implies that the corrections $(\bar{u}, \bar{v}, \bar{w})$ that must be added to the observed/interpolated field to satisfy Eq. (1) are irrotational, and thus calculable via a scalar potential, ϕ. However, the usual potential relationship, $\vec{\bar{u}} = \nabla\phi$, is modified as follows:

$$\begin{aligned} u &= u_i + \bar{u} \qquad & \bar{u} &= \tau_h \frac{\partial \phi}{\partial x} \\ v &= v_i + \bar{v} \qquad & \bar{v} &= \tau_h \frac{\partial \phi}{\partial y} \\ w &= w_i + \bar{w} \qquad & \bar{w} &= \tau_v \frac{\partial \phi}{\partial z} \end{aligned} \tag{38}$$

where τ_h, τ_v are termed the horizontal and vertical "transmissivity coefficients," respectively; appropriate values are to be determined empirically. This development ignores the fact that the analysis is being applied within the planetary boundary layer, where by definition viscous effects are rendered non-negligible owing to the strong gradients normal to the surface. Furthermore, the condition of irrotationality, $\nabla \times \vec{\bar{u}} = 0$, is not satisfied by Eq. (38) except in the special case $\tau_h = \tau_v$. Nevertheless, accepting this premise for the sake of argument, and substituting Eq. (38) into Eq. (1) results in the following partial differential equation for ϕ:

$$\frac{\partial}{\partial x}\left(\tau_h \frac{\partial \phi}{\partial x}\right) + \frac{\partial}{\partial y}\left(\tau_h \frac{\partial \phi}{\partial y}\right) + \frac{\partial}{\partial z}\left(\tau_v \frac{\partial \phi}{\partial z}\right) = -\left(\frac{\partial u_i}{\partial x} + \frac{\partial v_i}{\partial y} + \frac{\partial w_i}{\partial z}\right) \tag{39}$$

But Eqs. (38) and (39) are identical to Eqs. (32a)-(32c) and (33), respectively, if we make the identifications that $\tau_h \rightarrow 1/(2\alpha_1^2)$, $\tau_v \rightarrow 1/(2\alpha_2^2)$, and $\phi \rightarrow \lambda$. Thus the same set of equations is ultimately solved, regardless of the arguments used to derive them. The present author feels the variational calculus development is more defensible, and for that reason has included the NOABL model in this category.

The preceding paragraph makes clear that the Lagrange multiplier λ in Eqs. (36a)-(36c) and (37) can be interpreted as a potential ϕ in the special case $\alpha = 1$. The reader is cautioned that it is only the adjustment to the (initial) interpolated velocity field in Eqs. (36a)-(36c) that is correctly described as a potential flow. The full velocity field, which includes (u_i, v_i, w_i), will in general *not* be a potential (*i.e.*, irrotational) flow, *unless* the initial velocity field is itself irrotational. Ross, *et al.* (1988, 1991) correctly pointed out that for a uniform initial wind field, the solution of this system with $\alpha = 1$ will yield a potential flow solution. As a result some have come to regard the term "potential flow" as more or less synonymous with the choice $\alpha = 1$, with no consideration given to the initial field. On the contrary, in a field application where multiple observations are available from which to interpolate, it must be expected that the initial as well as the final adjusted wind fields will not be potential flows regardless of the value given to α.

The NOABL model (Traci, *et al.* (1978)) is unique in one other respect: it is the only model encountered in the literature that can solve the equations either in physical space, using an SST representation of the topography, or alternatively using TFC (*cf.* p. 5). The authors point out that the latter is the preferable approach, as it allows more precise imposition of the surface boundary condition, as well as variable grid spacing in the σ coordinate; the result is a more accurate and economical solution. For a more thorough discussion of this point, see the excellent review by Ratto, *et al.* (1994). The SST capability was nevertheless retained to increase flexibility and maintain compatibility with other physical-space-based codes.

The COMPLEX model (Bhumralkar, *et al.* (1980), Endlich, *et al.* (1982)) is closely related to MATHEW, and represents a brief, but apparently temporary, dalliance on Endlich's part with the variational calculus approach. (Recall from §2.2 that it was Endlich (1967) who pioneered the Point-Iterative scheme.) It was developed to aid in the siting of wind turbines by highlighting those areas where the terrain had the effect of enhancing the local winds. COMPLEX differs from MATHEW in two important respects.

The first has to do with the equations solved by COMPLEX; their derivation follows along the same lines as that presented above through Eqs. (32a)-(32d). But then, instead of eliminating *u*, *v*, and *w* in order to derive a single PDE for λ, Bhumralkar, *et al.* (1980) first eliminate *v*, *w*, and λ to get a single equation in *u* alone; then they eliminate *u*, *w*, and λ to get a single equation in *v* alone, *etc*. The end result is a separate three-dimensional PDE for each of the components *u*, *v*, and *w*, *i.e.*, the Lagrange multiplier λ is eliminated altogether. The three PDEs are solved using numerical relaxation techniques, and the results should be (except for discretization errors) equivalent to those obtained by solving Eq. (37) followed by (36a)-(36c) above. But why go to the added expense of solving three separate (albeit very similar) PDEs,

when the method described above requires the solution of only one PDE (as once λ is known, Eqs. (36a)-(36c) are essentially algebraic)? Bhumralkar, *et al.* never explain their motivation in this regard, nor do they discuss how they set boundary conditions for their equations. Nevertheless, it is interesting to note that each of their three PDEs contains only the single parameter $\alpha_1/\alpha_2 = \alpha$ (= $[W_H/W_V]^{1/2}$ in their notation). This further reinforces the argument made on p. 26, *i.e.*, that the solution for the wind field depends only on a single arbitrary parameter, α, not two. However, Endlich, *et al.* (1982) state that the values of $\alpha^2 = W_H/W_V$ "that give appropriate results are in the range 10^{-10} to 10^{-12}", which is orders of magnitude lower than those found appropriate in MATHEW (Sherman (1978)) or the ATMOS1 model (see below). The second respect in which COMPLEX differs from MATHEW is that it solves the TFC, as opposed to the SST, formulation of the equations, with the attendant advantages in accuracy and efficiency (*cf.* p. 28).

Endlich, *et al.* (1982) point out that the predicted flow around and over obstacles is sensitive to where the top of the computational domain is placed—typically at the top of the planetary boundary layer, or at the base of an elevated inversion. COMPLEX allows this height to vary spatially as well. As this is not a directly observed meteorological variable, it introduces another ambiguity into the use of the model. (Note, however, that this is true of *any* of the methods described in this report, and is not unique to the variational calculus approach.) Endlich, *et al.* (1982) and Endlich (1984) discuss at some length how they chose to parameterize the boundary layer thickness variations in terms of its average thickness, a minimum thickness, and a "slope factor". Ratto, *et al.* (1994) describe how other investigators have handled this question. This discussion is useful in and of itself, regardless of which approach is taken to satisfying Eq. (1).

ATMOS1 is a diagnostic model developed by Davis, *et al.* (1984) to provide meteorological inputs to ATMOS2, a pollutant advection/diffusion code. It is similar to MATHEW and NOABL, in that it solves a single PDE, Eq. (37), for the λ field, from which *u*, *v*, and *w* are then computed using Eqs. (36a)-(36c). The equations are written in terrain-following coordinates (TFC), and a SOR technique is again used to obtain the λ solution. Like Sherman (1978), Davis, *et al.* found that values of $\alpha^2 \sim 10^{-4}$ are appropriate for stable conditions, while for unstable conditions $\alpha^2 > 1$ will likely be necessary. A companion paper by King and Bunker (1984) in the same journal/issue compares the predictions of the ATMOS1/ATMOS2 models against measured concentration data. They conclude that while the diagnostic model gives reasonable accuracy over both simple and complex terrain, to significantly improve its predictions would require more finely resolved spatial observations, in addition to more knowledge of the vertical wind profiles.

Similar conclusions are drawn almost universally in the literature on diagnostic models, and serve as a reminder that minimizing the functional *E* in Eq. (28) does more than simply serve to enforce the continuity condition, Eq. (1). It also minimizes the mean-square difference between the observed/interpolated wind field from which the model starts, and the final adjusted wind field. *If the interpolated wind field has not been sampled at points sufficiently representative of the underlying terrain, there is little hope that the final winds will faithfully reflect its influence.*

The MINERVE model was developed by Geai (1987a,b)† of the French Electricity Board for use as a tool in the prediction of pollutant advection/diffusion. It too is based on the variational formulation described above, expressed in the TFC system. MINERVE interpolates the observed data to obtain the initial (u_i,v_i,w_i) field before minimizing the functional in Eq. (28). Various interpolation procedures are included as options, which can be selected based on the nature and distribution of the observations. To achieve reasonable fidelity, MINERVE is said to require a minimum of three surface wind observations and one vertical profile (Bradley, *et al.* (1997) and Cox, *et al.* (1998)). The system can be solved assuming either a constant α, as in Eqs. (36a)-(36c) and (37), or with α allowed to vary from point to point, as in Eqs. (32a)-(32c) and (33). Equation (33) or (37), as the case may be, is solved using SOR. As it has evolved over the years, MINERVE now allows the value(s) of α to be prescribed by the user, or calculated internally from empirical parameterizations related to atmospheric stability as discussed below (Cox, *et al.* (1998), Sontowski and Dougherty (1996)). Perhaps what most distinguishes MINERVE from other models in this category is the number of investigations in which it has been used, and the list of users it has attracted who were not involved in its original development. The studies have included comparisons with both wind tunnel data and atmospheric flows over complex terrain, and provide an extensive database from which to assess its accuracy. More will be said in this regard in §4.

NUATMOS is a model developed by Ross, *et al.* (1988). Like the earlier ATMOS1 (Davis, *et al.* (1984)) model on which it is based, NUATMOS employs TFC and variable grid spacing in the vertical coordinate. What most distinguishes it from earlier models is the authors' attempt to choose α based on objective criteria related to atmospheric stability. Heretofore, $\alpha = \alpha_1/\alpha_2$ had been chosen based primarily on the relative errors/uncertainty in the observed values of the horizontal *vs*. vertical wind components (*cf.* p. 21), or adjusted through trial-and-error until the solution looked appropriate. As both of these approaches involve a considerable element of subjectivity, and the choice has a significant influence on whether the adjusted flow goes around obstacles, or over them, there remained a strong motivation to objectify this part of the analysis. It was already known that: $\alpha \sim 1$ would allow more or less equal adjustments in the horizontal and vertical components of the wind in order to minimize Eq. (28), and hence was appropriate to neutrally-stratified flow; $\alpha < 1$would result in larger changes to the horizontal components than the vertical component, and so is appropriate to stable flows; and $\alpha > 1$ would emphasize changes in the vertical component, and hence should be used for unstable flows. But that still left considerable latitude to the user.

Starting from conservation of energy arguments, Ross, *et al.* (1988) developed the following parameterization of α in terms of the Froude number, *Fr*:

$$\alpha^2 = \begin{cases} 1 - \dfrac{a}{\sqrt{Fr}} & z > H_c \\ 0 & z \le H_c \end{cases} \qquad \text{for } Fr > 0.5 \tag{40}$$

†As of this writing, the present author has been unsuccessful in obtaining either of these two reports. The description that follows must of necessity rely on the publications of others.

where $Fr = U_\infty/(Nh)$ is the Froude number characteristic of an isolated obstacle, such as a hill; U_∞ represents the assumed uniform background velocity; h is the characteristic height of the hill; $N = [(g/\theta)(\partial\theta/\partial z)]^{1/2}$ is the Brunt-Väisälä frequency appropriate to $\partial\theta/\partial z \geq 0$; g is the gravitational acceleration; and θ is the potential temperature (see, *e.g.*, Panofsky and Dutton (1984)). H_c is the upstream height of the so-called "critical streamline": below H_c the flow has insufficient energy to surmount the obstacle, and so passes around it, whereas above this level the flow has sufficient strength to pass over it. Hunt and Snyder (1980) suggest using

$$H_c \geq h(1 - Fr) \tag{41}$$

for stable and neutral conditions.

By comparing solutions obtained using NUATMOS for various constant values of α against the experimental data of Hunt and Snyder (1980) for flow over an isolated three-dimensional hill, an appropriate value for the empirical constant, a, was determined. It was found that $a \cong 0.7$ gave reasonable agreement, provided $Fr > 0.5$; for values below this Eq. (40) predicts negative values, which is physically unrealistic. Ross, *et al.* (1988) conclude that this result provides an adequate description of the functional relationship $\alpha^2(Fr)$ for the simple topography and uniform background flow for which the experiments were conducted, and for both neutrally-stratified and stable conditions. They caution, however, that the "best fit" a may vary with the experiment, and even be a function of Fr—*i.e.*, the functional form in Eq. (40) may not be universal. And for complex terrain, it may even be necessary to let $\alpha = \alpha(x,y,z)$ throughout the domain.

Subsequently, Ross and Fox (1991) and Ross and Smith (1991) proposed that, based on additional laboratory data, Eq. (40) be replaced by:

$$\alpha^{-2} = 1 + \frac{3}{(S^2 - 1)Fr^2} \qquad \text{for } Fr \geq 0 \tag{42}$$

where the terrain-induced "speedup", S, is defined as U_{max}/U_∞ as obtained by first running NUATMOS with $\alpha = 1$. This too should only be applied to neutral and stable conditions. They conclude that, compared to using a uniform flow assumption everywhere in the field, progressively better comparisons with measured pollutant concentration data are obtained by: 1) correcting for changes in terrain elevation only using $\alpha = 1$; 2) choosing $\alpha = \alpha(Fr)$ as in Eq. (42) to reflect atmospheric stability; and 3) empirically choosing α to match the observed height, H_c, of the critical streamline. The last option assumes of course that such data are available, and there is sufficient time for the trial-and-error runs needed to do the match-up.

Moussiopoulos and Flassak (1986) developed two codes, CONDOR and REDBL, for diagnostic wind modeling. They derived their equations using potential flow arguments similar to Traci, *et al.* (1978), but acknowledge that the resultant system of equations is identical to that obtained from a variational formulation. Both codes are formulated using a standard TFC transformation, though the authors go into more detail in this regard than most. Their primary goal was to speed up the calculations by replacing the traditional SOR solution of the PDE for λ with more modern techniques that lend themselves to computers with vector architectures.

CONDOR makes use of a fast direct elliptic solver based on Fast Fourier Transforms (FFTs), coupled with a block-iterative technique to solve what amounts to Eq. (37) for $\alpha = 1$ in transformed coordinates. REDBL instead uses two interlaced cartesian grids of "red" and "black" points (hence the name) to modify the SOR method in such a way that it can be vectorized. (The standard SOR doesn't vectorize well because of the way data dependencies propagate during the iterations—*cf.* their Eq. (35).) Both codes were applied to adjusting the wind field over Athens, Greece using the same 3D grid and observed/interpolated data. The area covered was 55×55 km, with the upper boundary at a fixed height of 3 km with a mesh of $21 \times 21 \times 11 = 4851$ grid points. The solutions agreed well with one another, as they should, and were in reasonable agreement with a more sophisticated prognostic model. REDBL took ~ 250 ms, and CONDOR ~ 300 ms—*i.e.*, less than one second each—on the vector machine CYBER 205 to compute one mass-consistent flowfield. For comparison, both codes were also run on a conventional scalar processor (a SIEMENS 7881), and the run times increased by a factor of ~ 25.

The calculations by Moussiopoulos and Flassak (1986) appear to be all for $\alpha = 1$. Moussiopoulos, *et al.* (1988) later improved the CONDOR model in two important respects. First, the block-iterative technique was replaced with a Conjugate Gradient method which the authors claim significantly reduced the number of iterations needed for convergence. Secondly, the system of equations was generalized to allow for arbitrary α[†], and an attempt was made to objectively parameterize the latter in terms of the stability condition. Rather than relate α^2 to the Froude number *Fr*, as was done by Ross, *et al.* (1988, 1991), Moussiopoulos, *et al.* chose instead to work with the Strouhal number, *St*. For neutral and stable conditions, $St = 1/Fr$, with *Fr* as defined on p. 30. Following energy conservation arguments similar to those used by Ross, *et al*. (1988), and also comparing with the experiments of Hunt and Snyder (1980), Moussiopoulos, *et al.* (1988) suggest the following alternative to Eqs. (40) and (42):

$$\alpha^2 = 1 - \frac{St^4}{2}\left[\sqrt{1 + \frac{4}{St^4}} - 1\right] \qquad \text{for } St \geq 0 \tag{43}$$

This result yields the correct limits for both neutral ($St \to 0$, $\alpha^2 \to 1$), and highly stable ($St \to \infty$, $\alpha^2 \to 0$) conditions.

Moussiopoulos, *et al.* (1988) then went one step further and considered how α^2 might be parameterized for unstable conditions, $St < 0$. In this regime, $St = -h/(U_\infty \tau)$, where $\tau^{-1} = \sqrt{-(g/\theta)(\partial\theta/\partial z)}$ for $\partial\theta/\partial z < 0$; the quantity τ which replaces N^{-1} can be thought of as the characteristic buoyancy time scale. As there was no experimental data for unstable conditions to serve as a guide, they sought to bracket the range of values that α^2 might take. It seems reasonable to expect that the minimum would correspond to the value appropriate to neutral conditions, $\alpha^2 = 1$. For the maximum, they postulated the inverse of the value computed from Eq. (43) for -*St*. That is,

---

[†]Their Eqs. (6a)-(6c) differ slightly from the present Eqs. (36a)-(36c) because Moussiopoulos, *et al.* chose to set $\alpha_1^2 = 1/2$, whereas we followed Ross, *et al.* (1988) in setting $\alpha_1^2 = 1$. For the reasons cited on p. 26, this only affects the λ-field; the velocity field computed from either system will be the same provided the same ratio $\alpha_1/\alpha_2 = \alpha$ is used in both.

$$\alpha^2_{min} = 1 \qquad \text{for } St < 0$$
$$\alpha^2_{max} = \frac{1}{\alpha^2(-St)} \tag{44}$$

Equations (40), (43), and (44) are all plotted *vs*. *St* in Fig. 3 below. (Equation (42) was not included as it requires additional calculations to determine the speedup factor, *S*, for some specified terrain variation.) For *St* > 0, Eq. (43) provides a smoother transition at the neutral

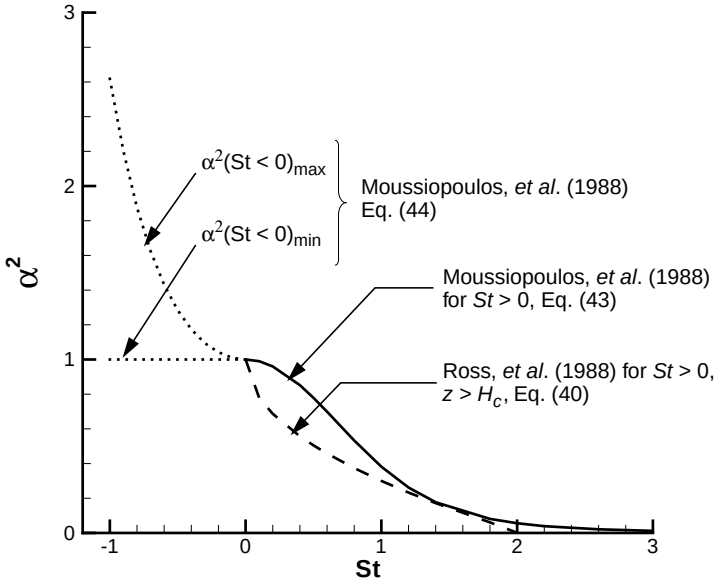

Figure 3. Parameterization of α^2 as a Function of Strouhal Number, *St*

condition, *St* = 0, and approaches zero only asymptotically as $St \rightarrow \infty$, whereas Eq. (40) is only valid between $0 \le St \le 2$. To judge which is more accurate would require that both be applied to the same dataset, and the results compared; to the author's knowledge, no such comparison is available.

The true variation of $\alpha^2(St < 0)$ is not known, but is expected to lie between the min/max limits shown. Moussiopoulos, *et al.* (1988) applied the updated CONDOR model to the wind field in the vicinity of Athens, Greece, with α allowed to vary with position throughout the 3D grid. One set of simulations was run using $\alpha = \alpha_{min}$ from Eq. (44), and another using $\alpha = \alpha_{max}$, in those regions where *St* < 0; such conditions were confined to the bottommost (*i.e.*, surface) layer in the domain. Both calculations used Eq. (43) when the local $St \ge 0$. Overall, the adjusted wind fields were found to be a good approximation to the actual winds, provided the observed/ interpolated data were sufficiently representative of the terrain. Surprisingly, the authors found only small differences in the (unstable) surface layer predictions between the two simulations, which they attribute to this layer being rather shallow. They conclude that, while further effort should be expended in developing a functional relationship for $\alpha^2(St < 0)$, the resulting predictions are not likely to be heavily influenced by the particular choice. The present author feels the latter conclusion is premature, based as it is on a single investigation, which underscores even more the need for further data and study regarding unstable conditions.

Venkatesan, *et al.* (1996, 1997) describe a diagnostic model named WIND04, which is part of a larger suite of codes called the System for Prediction of Environmental Emergency Dose Information (SPEEDI). It is similar to MATHEW (Sherman, (1978)) in that an SST representation of the topography is used, but differs from it in that α is allowed to vary, in the vertical direction only, according to Eq. (43) to reflect atmospheric stability. The authors conclude that replacing the SST representation with a TFC mapping would likely improve the model's predictions.

All the above models employ Finite-Difference (FD) approximations to solve the system represented by Eqs. (36a)-(36c) and (37) (or Eqs. (32a)-(32c) and (33)). Montero, *et al.* (1998) appear to be the first to develop a Finite-Element (FE) procedure for this problem, which forms the basis for their MEM3D model. The surface terrain is modeled as a collection of convex polyhedra, stored as a series of vertices, edges and surfaces. The interior volume of the computational domain is discretized using tetrahedral elements, with variable node spacing in the vertical direction to allow higher node densities near the surface. The other significant difference is the replacement of the traditional SOR iterative technique with the more modern BiConjugate Gradient Stabilized (Bi-CGSTAB) method. Two sample problems are solved, one with 4,608 nodes and 22,506 tetrahedra, the other with 6,662 nodes and 26,183 tetrahedra. Both used constant values for $\alpha \sim O(1)$, and consumed ~ 3 min of CPU time to adjust the wind field, which is a bit on the high side in comparison with other models.

Whether for this or some other reason, Montero and Sanin (2001) later abandoned the FE procedure, and reverted to the use of a FD model. They formulate their equations using TFC, and go into considerably more detail than other authors regarding the specific difference approximations that they used. The same choice of iterative solvers used in MEM3D was implemented, *i.e.*, Bi-CGSTAB with either Jacobi, SSOR, or ILU preconditioning. The wind field over a portion of one of the Canary islands was modeled at various times using a $51 \times 51 \times 14$ mesh, again using a constant value for $\alpha \sim O(1)$. No run times are reported.

Many investigators have noted that the adjusted wind fields resulting from the variational approach can be sensitive to the value chosen for α. Barnard, *et al.* (1987) sought to remedy this by determining what they claim is an 'optimum' α. Their procedure assumes that observations at multiple stations, eight or so for the calculations in their paper, are available. The wind field is initialized using only one of these; the remainder are withheld for use as "tuning" stations. An optimization procedure is used to drive numerous calculations with the NOABL model using various values of α to adjust the winds, and for each the root-mean-square error between the adjusted values computed at the tuning stations and the withheld observations is computed. The 'optimum' value of α is that which minimizes this r.m.s. error. A typical run time to determine this value using a VAX 11/780 computer is said to be about one-half hour. Such a procedure begs the question: since the variational method used in NOABL already minimizes the mean-square error between the adjusted and interpolated fields based on the observations it is given, wouldn't it be simpler to just provide all the available observations at the outset? That is, perhaps the sensitivity of the adjusted wind field to α could more easily be reduced by simply using more observations; the latter should improve the fidelity of the interpolations, and presumably require adjustments of smaller magnitude.

This is the tack taken by Harada, *et al.* (2000), who also sought to reduce the ambiguity in choosing α. Actually, the problem they set about solving is even more general, in that they did not assume equal weights premultiplying *u* and *v* in Eq. (28), but rather assigned unique factors α_u, α_v, and α_w to each component. Thus, the functional they seek to minimize is given by,

$$E(u, v, w, \lambda) = \int_V \Big[\alpha_u^2 (u - u_i)^2 + \alpha_v^2 (v - v_i)^2 + \alpha_w^2 (w - w_i)^2 + \lambda \left(\frac{\partial u}{\partial x} + \frac{\partial v}{\partial y} + \frac{\partial w}{\partial z} \right) \Big] dx dy dz \tag{45}$$

This leads to a system of equations identical to Eqs. (32a)-(32d), but with α_1, and α_2 replaced by α_u, α_v, and α_w in the first three of these equations, respectively. The PDE for λ that results now contains all three factors as well, but otherwise the procedure for solving for λ, *u*, *v*, and *w* is completely analogous to that already described. As before, this minimizes the mean-square deviation between the *adjusted* and *interpolated* wind fields, while enforcing mass conservation. In contrast to Barnard, *et al.* (1987), Harada, *et al.* use all available observations to initialize their calculations. They set $\alpha_u = 1$, and then seek those values of α_v and α_w which minimize the mean-square difference between the *adjusted* and *observed* values.

A genetic algorithm (GA) is employed to find these optimum values. GAs are one branch of the fertile area of computational research known as artificial intelligence, and are too far afield from the present subject to go into much detail here. Suffice it to say that they artificially mimic the processes of natural selection, evolution, and Darwin's principle of survival of the fittest to arrive at an optimal solution. Harada, *et al.* present results for only two cases, both concerned with the flow about Waita mountain in Japan. In both cases the optimum values for α_w were quite high and nearly equal, ~ 52-53; this might have been anticipated, as in both cases the atmosphere was very stable. Curiously, the values found for α_v in each case differed considerably, 0.7 *vs*. 1.1. The authors speculate this may have been due to there being significantly different ambient wind directions in the two cases. It is too soon to tell, based on just these two cases, whether their generalization to $\alpha_v \neq \alpha_u$ represents a significant improvement or not. Unfortunately, no results for which the genetic algorithm was not used (*e.g.*, with $\alpha = \alpha_1/\alpha_2 = \alpha_v/\alpha_w$ chosen from stability considerations as proposed by Ross, *et al.* (1988, 1991) or Moussiopoulos, *et al.* (1986, 1988)) are presented for comparison, and no run times are quoted, so it is difficult to gauge whether the additional effort spent on optimization is warranted.

Mathur and Peters (1990) suggest several ways to improve on the variational formalism. After the winds have been adjusted according to the systems represented by either Eqs. (33), (32a)-(32c), or Eqs. (37), (36a)-(36c), Direct-Differencing can be applied to the horizontal (*u*,*v*) field to further correct the *w* component. As this involves no iterations, it can be performed very quickly. According to the authors, this results in smoother *w* variations with far less irregularities, and more reasonable magnitudes, than would be obtained by differencing the initial interpolated field. Recall from §2.1 that Direct-Differencing the interpolated field can lead to *w* values of unreasonably large magnitude unless the interpolated field is known to high accuracy. The lower magnitudes for *w* obtained from Mathur and Peters' suggestion are the result of having already removed much of the divergence before doing the differencing. A second benefit is that any residual divergence left after the variational adjustment is further

reduced, typically by several orders of magnitude. In a published comment on the Mathur and Peters paper, Ross and Smith (1991) point out that the same result could have been obtained by simply continuing the iterative solution in the variational adjustment to a tighter convergence criterion. This highlights a question that still appears not to have been resolved in the open literature: how small a level can the divergence be driven to by use of the Variational Calculus approach? Sherman (1978) claims reductions of twelve orders of magnitude, while Mathur and Peters (1990) and Kitada, *et al.* (1983) were only able to achieve reductions of between one and two orders of magnitude, and found that it depended on the value chosen for α. More controlled numerical experiments are clearly needed to resolve this issue.

Mathur and Peters also show how the variational formalism can be extended to include conservation of the vertical component of vorticity in the interpolated field, in addition to vanishing divergence. Recall that these are the same conditions satisfied by the Point-Iterative approach (p. 9). Based on their numerical results using such a generalized scheme they conclude, however, that the additional constraint has an insignificant effect on the final results, and so is probably not worth the extra effort required. Ross and Smith (1991) subsequently pointed out that *the vertical component of vorticity is automatically conserved by the variational adjustment*, without any need to specify it as a separate constraint, if equal (constant) weight factors are used for both *u* and *v*. This is easily seen by substituting Eqs. (32a) and (32b) into the definition of the vertical component of vorticity, Eq. (9):

$$\omega = \frac{\partial v}{\partial x} - \frac{\partial u}{\partial y} = \left(\frac{\partial v_i}{\partial x} - \frac{\partial u_i}{\partial y}\right) + \frac{1}{2\alpha_1^2}\left(\cancelto{0}{\frac{\partial^2 \lambda}{\partial x \partial y} - \frac{\partial^2 \lambda}{\partial y \partial x}}\right) = \omega_i \tag{46}$$

i.e., Mathur and Peters' numerical results simply confirm a side benefit of the procedure that can be demonstrated analytically. Indeed, Ratto, *et al.* (1994) note further that if $\alpha_1 = \alpha_2 =$ constant, and λ is suitably well-behaved, all three components of vorticity will be preserved.

For most applications, the incompressible form of the continuity equation, Eq. (1), is adequate. However, for situations where the density may vary spatially but not in time, *e.g.*, very large domains, or when significant heat sources or sinks are present that can produce strong temperature differences, the so-called "anelastic" form of the equation,

$$\nabla \cdot (\rho \vec{u}) = 0 \tag{47}$$

is more appropriate (Ratto, *et al.* (1994)). Mathur and Peters (1990) show how this can be used to replace Eq. (1) as the strong constraint in the variational analysis as well. Unfortunately, no predictions based on such a scheme are presented. Though the analysis presented by Endlich, *et al.* (1982) employs Eq. (1), those authors claim to have performed calculations for spatially-varying ρ, without providing any details. They report that differences between these results and those predicated on constant ρ were "barely detectable."

It is clear that, of the four approaches to adjusting wind fields so as to satisfy mass conservation that have been proposed, that based on the calculus of variations has attracted by far the most followers. No doubt this is due to its unified treatment of all three wind components simultaneously, and relative lack of ambiguity. Indeed, the only significant ambiguities in the

use of this method are: 1) whether to allow α_1 and α_2 to vary independently or to assume—as apparently most investigators do—a constant value for $\alpha = \alpha_1/\alpha_2$; and 2) how values for these Gauss precision moduli/weighting factors/transmissivity coefficients are to be specified. More data are needed, and much work remains to be done, on the question of whether a universal parameterization of $\alpha^2(St)$, or $\alpha^2(Fr)$, can be developed that covers the gamut from stable to neutral to unstable conditions, or whether some other approach is needed. Another potential drawback to this approach is the necessity of using an iterative scheme to solve Eq. (33) or (37), with the attendant questions of convergence and robustness such a technique entails. But the large community of users suggests that this is not a significant problem, and reported run times on the order of a few minutes are well within the bounds of what is required of "real-time" models.

Intentionally Left Blank

3. LINEARIZED MODELS

In contrast to the diagnostic, or mass-consistent, models of §2, which seek only to satisfy the continuity condition, the class of methods known collectively as linear or linearized models attempt to solve the steady-state momentum equations as well. Because the terms "linear" and "linearized" are so common in many branches of science and mathematics, attempts to cull the literature using SciSearch® were not very productive, even when restricted to the disciplines of meteorology and atmospheric sciences. As a result, most of the publications listed beginning on p. 61 were identified in a bootstrap manner from citations given in those already at hand. There is the risk that any such bibliography is more inbred, and less up-to-date, than would otherwise have been the case, but it is the author's opinion that the list is fairly representative nonetheless.

Linear models tend to follow, at least in broad outline, a more uniform methodology than do the diagnostic models; most of the differences between them lay in the details. Owing partially to this, but primarily to the fact that they are not as well-suited to the NEST group's applications as the diagnostic models (for reasons cited below), the discussion in this section will not go into as much depth as that of §2.

The seminal paper in this branch of wind modeling, to which all the various linear models appear to trace their origin, is that by Jackson and Hunt (1975). The problem studied is that of *two-dimensional* incompressible *adiabatic* flow over a *uniformly rough* surface on which is situated an *isolated low* hill, as sketched in Fig. 4. Far upstream of the hill the oncoming wind

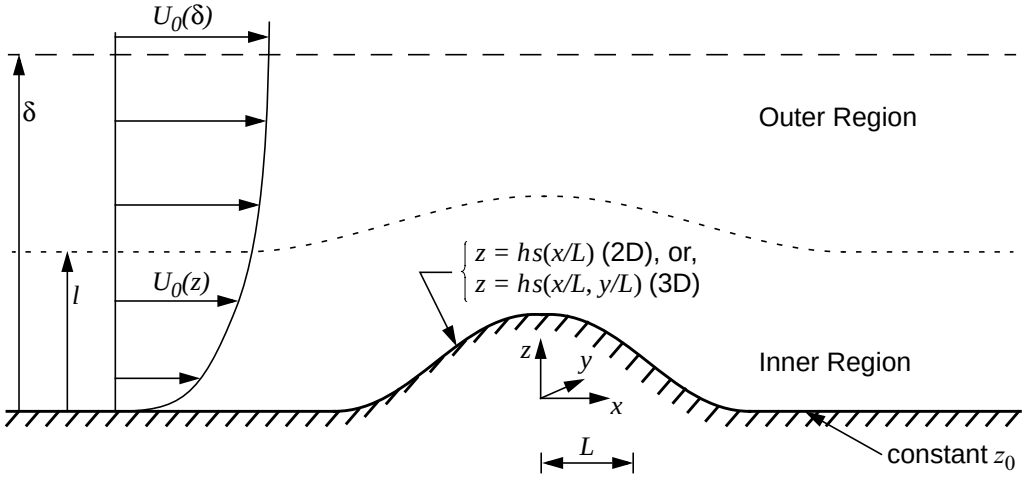

Figure 4. Linearized Model of Flow Past an Isolated Hill

is assumed horizontal, unidirectional (aligned with the x-axis), and a function of height only, $w(x,z) = 0$, $u(x,z) = U_0(z)$[†], with a variation that can be described by a logarithmic profile. The hill profile is specified analytically in the form $z = hs(x/L)$, where h is its height, $0 \le s(x/L) \le 1$, and $s \to 0$ as $x/L \to \pm\infty$. L is a characteristic length, which they define as that distance from the

[†]The notation used in this section differs somewhat from that employed by the authors cited to maintain consistency with the rest of the report.

peak at which $s(x/L) = 0.5$ (p. 942). The following is an attempt to list the key approximations/ steps in the analysis without getting mired in the details:

1. The underlying premise is that the flow throughout the computational domain can be viewed as a small perturbation about the oncoming, undisturbed flow. That is, if (u, w) and (u', w') represent the total and perturbation velocity components, respectively, *i.e.*,

$$\begin{aligned} u &= U_0 + u' \qquad & u'/U_0 &\ll 1 \\ w &= w' & w'/U_0 &\ll 1 \end{aligned} \tag{48}$$

   This allows any nonlinear terms in the equations to be replaced by ones with either constant coefficients, or at worst, coefficients whose variation with the independent variables is known *a priori*. The equations are thus rendered linear, and hence the name. The small-perturbation assumption requires that the hill be low and of moderate slope, *i.e.*, the analysis is strictly valid only for

$$\frac{h}{L} \ll 1 . \tag{49}$$

   It is worth noting here that the continuity equation, Eq. (1), is already linear by virtue of having assumed incompressible flow. Hence, it is only the momentum equations, notably the advective terms, which are nonlinear and necessitate this restriction.

2. The energy equation is not considered. This is apparently the reason for having assumed the flow to be adiabatic at the outset. As a result, the solutions can be expected to be valid only for flows that are neutrally stable, or nearly so. (Subsequent investigations relaxed this restriction—*cf.* p. 43 below.)

3. The roughness length, z_0, is assumed to be constant and to satisfy

$$\frac{L}{z_0} \gg 1 . \tag{50}$$

4. A simple mixing length model is used to achieve closure of the equations—*i.e.*, the otherwise unknown turbulent Reynolds stresses are modeled as algebraic functions of the mean velocity gradients.

5. A Fourier transform is applied to the linearized equations[†] with respect to the horizontal coordinate, in this case x. This has two primary effects on the equations. Let $F(x,z)$ represent any of the unknown perturbation quantities, whether velocity or pressure. After the transformation, it is replaced by its Fourier transform, $F(k,z)$, where k is the corresponding wavenumber. The second change effected by the transform is that any differential operations with respect to x will have been replaced by an algebraic dependence on k. The original system of partial differential equations (PDEs) is thus transformed to a system of ordinary differential equations (ODEs) in z. *Appendix A* gives more details regarding the Fourier transformation, including the reason for requiring that the disturbance, *i.e.*, the hill, be isolated.

[†]For this reason models in this category are sometimes referred to in the literature as “linearized spectral” or “spectral diagnostic” models.

6. With further simplifying assumptions the ODEs admit families of relatively simple analytical solutions. The solution for a particular case is rendered unique by imposing suitable boundary conditions that fix what amount to the constants of integration. To avoid imposing arbitrary boundary conditions on the transforms of velocity or pressure, the boundary layer is divided into an outer region, which is essentially inviscid, and an inner layer of thickness l (Fig. 4) where turbulence is significant. The magnitude of l is determined by balancing the competing acceleration and stress gradient terms in the inner layer.

7. If z_{in} and z_{out} denote (suitably-scaled) transformations of the independent coordinate z in the inner and outer regions, respectively, the solution in the inner region is required to satisfy the no-slip surface boundary condition as $z_{in} \rightarrow 0$, while that in the outer region must approach the freestream conditions at the boundary-layer's edge as $z_{out} \rightarrow \infty$. In addition, the inner solution for $z_{in} \rightarrow \infty$ is asymptotically matched to the outer solution for $z_{out} \rightarrow 0$.

8. Upon completing Step 7, transforms $F(k,z)$ for all the various perturbation fields are known in both the inner and outer layers. The physical fields $F(x,z)$ are then obtained from the inverse transform (Eq. (51b) in *Appendix A*), and after adding back in the undisturbed flow, analytical results are obtained across the entire boundary layer.

For a thorough discussion of all the assumptions and approximations, the reader should consult Jackson and Hunt (1975). The authors compare their results against both wind tunnel flows and whatever applicable real world data they could find. The comparisons are encouraging, if somewhat limited.

Later investigations extended the Jackson and Hunt (1975) model in several respects, and are discussed below. It should be noted that in many of these investigations the results are able to be expressed analytically only as far as the solutions of the ODEs for the transforms of the perturbation functions (Step 7 above). Numerical techniques, *i.e.*, Fast Fourier Transforms (FFTs) must then be employed to evaluate the inversion integrals (Step 8). Nonetheless, results can still be obtained in considerably less time than would be required by a full-blown numerical solution, *i.e.*, one based on a finite-difference or finite-element model of the full PDEs.

Mason and Sykes (1979) expanded the applicability of the Jackson and Hunt model by generalizing it from two to three dimensions. The principal difference is having to perform Fourier transform/inverse operations with respect to both x and y, *i.e.*, in Steps 5 and 8 above, $F(x,z) \rightarrow F(x,y,z)$ and $F(k,z) \rightarrow F(k_1,k_2,z)$, where k_1 and k_2 are the wavenumbers in the x and y directions, respectively. The authors highlight the qualitative nature of the differences between the two- and three-dimensional solutions, and compare the latter against experimental data obtained from Brent Knoll. The Mason and Sykes model was also programmed independently and subjected to further validation study—though still for "isolated" features—by Taylor and Walmsley (1981) and Walmsley and Taylor (1981).

Carruthers and Choularton (1982) presented a semi-analytical theory for two-dimensional airflow over an isolated hill. The boundary layer is still assumed to have neutral stratification, but is capped by an elevated inversion layer. They found it advantageous to divide the flow into three distinct layers, and rather than working with primitive variables (pressure, velocity),

instead solve the linearized vorticity equation. Comparisons with observations made on Great Dun Fell were encouraging.

The problem with applying either the 2D Jackson and Hunt (1975) or 3D Mason and Sykes (1979) theories to real applications is that they assume an isolated disturbance, surrounded by a uniform plain extending to infinity. Even the authors admit to having difficulty finding appropriate validation data (*cf.* pp. 950-951, and pp. 388-389, respectively). The first investigation that attempted to apply linear theory to "real world" terrain of finite extent was that of Walmsley, *et al.* (1982). They used essentially the Mason and Sykes analysis, but with the region of interest, of dimension L_R say, surrounded by a flat plain of uniform roughness and size $L > L_R$. This pattern is assumed to repeat itself periodically in both *x* and *y,* as shown schematically in Fig. 5, where the periodicity in *y* is not shown for reasons of space. We have

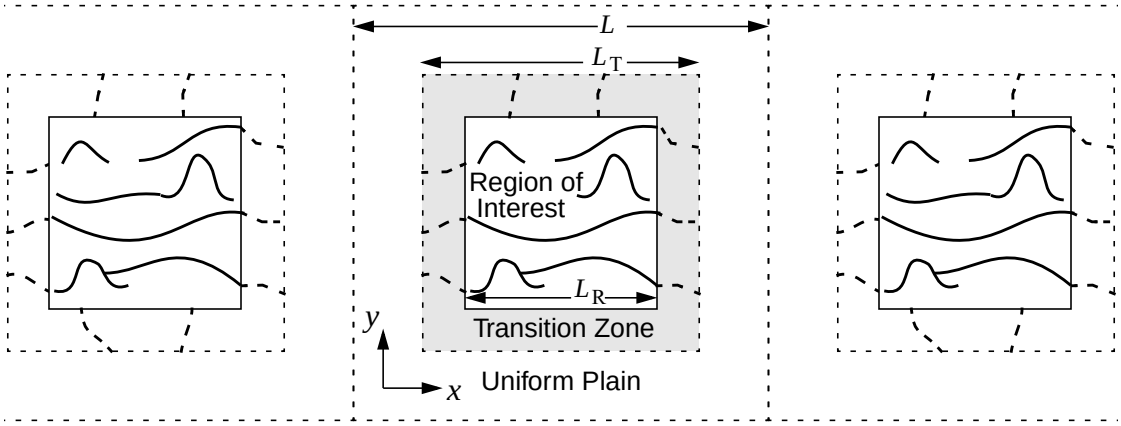

Figure 5. Imagined Periodic Terrain Variation Assumed by Linear Theory

assumed for simplicity that the horizontal footprint is square, though the analysis is applicable to arbitrary aspect ratios. The ratio L/L_R is set sufficiently large that periodic lateral boundary conditions can be imposed without unduly influencing the flow within the region of interest.

However, if the terrain at the edges of the inner region were to change abruptly from its actual elevation to that of the surrounding plain, spurious high-frequency oscillations would result in the solution. For this reason, a transition zone is inserted between the real terrain and the surrounding plain, within which the elevation is allowed to blend smoothly between the two. This introduces an additional parameter, the ratio L_T/L_R. Finally, Walmsley, *et al.* (1982) use discrete Fourier series to transform the PDEs to ODEs, rather than infinite Fourier transforms, as the former are more appropriate to periodic, as opposed to isolated, disturbances (*cf. Appendix A*). The spectral content of the resulting solutions will depend to some degree on the parameters L/L_R and L_T/L_R. Presumably, as these ratios increase, the solution in the region of interest will converge to one that is unaffected by the artificial periodicity or the transition zone. However, to the author's knowledge, no one has yet performed a systematic study of how large L_T/L_R and L/L_R must be before the solution within the region of interest stops changing.

Walmsley, *et al.* (1982) refer to the model described above as MS3DJH/1 (Mason and Sykes Three-Dimensional Extension of the Jackson and Hunt theory/Version 1). Its predictions are said to overemphasize the influence of small-scale (high wavenumber) topographic features.

They found that smoothing the terrain reduced the level of such 'noise', but were unable to derive well-founded criteria for when the smoothing should be applied. A modified model, dubbed MS3DJH/2, was developed which they felt more accurately depicted the effects of such features. Its predictions agree well with MS3DJH/1 near the ground, but the high wavenumber content of the solution decays more rapidly with height. There is a cost, however: for the same $256 \times 256 \times 3$ grid, MS3DJH/1 consumed ~ 1 minute of CPU time, *vs*. 20 minutes used by MS3DJH/2.

Another drawback to the application of the earlier analyses is the need to choose a single characteristic length scale L (*cf*. Fig. 4). Taylor, *et al.* (1983) note that, while the predictions of MS3DJH/1 and MS3DJH/2 are not unduly sensitive, the model results nevertheless do depend on the choice of L. For very simple terrain features, various alternative definitions may give similar results; but for complex topography, the choice may not be clear. The argument is made that what is needed is a wavenumber-dependent scaling of the underlying length and velocity scales. The authors point out that, rigorously speaking, such a change would require that terms through first-order in the Jackson and Hunt/Mason and Sykes analysis be kept, whereas MS3DJH keeps only the zeroth-order terms. Hence, this must be viewed as a heuristic or *ad hoc* modification to the model. Another change introduced by Taylor, *et al.* (1983) is to improve the matching of the horizontal perturbation velocity between the inner and outer layers, so that a single 'universally-valid' expression results. Both these changes are incorporated in the next-generation model, MS3DJH/3.

Mason and King (1985) independently developed similar refinements to the linear theory, notably the use of uniformly valid solutions and distinct velocity scales appropriate to the inner and outer layers. They also go into somewhat more detail regarding the sizes chosen for the overall (periodic) domain and the transition zone relative to the region of interest (*cf*. Fig. 5), *viz*., $L_T/L_R = 1.14$ and $L/L_R = 3.66$. It is not clear why these particular values were chosen, or whether a systematic study of the effects of varying these ratios was carried out. Results showed improved agreement with nonlinear finite-difference calculations, and trends similar to those seen by Taylor, *et al.* (1983).

The above studies were all for neutrally stable flows. Hunt, *et al.* (1984, 1988a, 1988b) also continued with the development of linearized theories, notably considering the effects of various degrees of stratification and different oncoming flows. They retain the concept of inner and outer regions (*cf*. Fig. 4), but further refine the model as follows. The outer region is subdivided into an upper and a middle layer, while the inner region is subdivided into a shear-stress layer and an inner surface layer (Hunt, *et al.* (1984, 1988b)). Analyses are presented for stably stratified flows assuming a logarithmic oncoming profile (1988a), and for neutrally-stable flows in which the oncoming flow is allowed to have either a logarithmic, power-law, or linear profile with height (1988b).

Belcher, *et al.* (1990) considered the effects of (one-dimensional) changes in surface roughness on the flow, in the context of a two-dimensional flow model. Walmsley, *et al.* (1986) extended the analysis of Taylor, *et al.* (1983) to include two-dimensional variations in surface roughness in a three-dimensional flow model, again assuming neutral stratification. This incarnation is designated MS3DJH/3R. Carruthers, *et al.* (1988) employed a model which divides the turbulent boundary layer into three sub-layers: the inner, middle, and upper layers.

Drawing on the ideas put forth in several earlier investigations, their model, dubbed FLOWSTAR I, incorporates the effects of various stratifications, oncoming wind profiles, and changes in both surface elevation and surface roughness. FLOWSTAR I is said to be able to calculate the flowfield at a single height on a 32×32 horizontal grid in ~ 10 min using an IBM PC/AT. Later improvements were added, resulting in the FLOWSTAR III model (Finardi, *et al.* (1993)).

Researchers at the Risø National Laboratory in Denmark have also been active in this branch of wind modeling. Astrup, *et al.* (1997) describe their independent development of a linear model that is capable of treating inhomogeneous surface roughness. Their model is incorporated as part of the LINCOM code, which is also capable of predicting the effects of surface elevation changes and thermal stratification. LINCOM is part of a preprocessor chain known as MET-RODOS, which provides meteorological inputs to a yet larger collection of codes, RODOS (Real Time On Line Decision Support), assembled to calculate the atmospheric transport and dispersion of radioactive materials (Mikkelsen, *et al.* (1997), Astrup, *et al.* (2001)).

As noted above, several models purport to include the effects of thermal stratification. Typically, this involves modeling its effects in some empirical manner, since linear models ordinarily make no attempt to satisfy energy conservation locally. An important exception is the work by Troen and de Baas (1986). Their "simple" model for three-dimensional neutrally stable flow (*cf.* their §2.1 and 2.2) is the basis on which LINCOM computes the effects of topographic variations, according to Astrup, *et al.* (1997). However, Troen and de Baas take the linearized analysis a step further in what they term the "generalized" model (their §2.4). The set of equations on which this model is based includes both the energy equation and Coriolis terms. They claim this can be done "without further assumptions and without seriously complicating the mathematics". To the present author's knowledge, the generalized linear model of Troen and de Baas (1986) is unique in this regard. However, their paper presents only very limited numerical results and no comparisons with experiment for the generalized model. Moreover, Astrup, *et al.* (1997) and Mikkelsen, *et al.* (1997) seem to imply that theories other than Troen and de Baas' are currently used to model thermal effects in LINCOM. It would appear that the accuracy and practicality of including the energy equation in such models is still an open question.

It is sometimes claimed that linear models have a speed advantage over diagnostic models (Troen and de Baas (1986)). No solid evidence to support this claim was found. True, most diagnostic models involve an iterative process of some sort to adjust the wind field, whereas linear models require no iterations; their results are typically expressed analytically up to the last step, where the final fields are formed using inverse Fast Fourier Transforms (FFTs). Hence, it may well be that the CPU time per grid point is less for linear than for diagnostic models. But CPU time per grid point is not the appropriate metric to use when making such comparisons, because it ignores the fact that linear models surround the region of interest with flat terrain and a transition zone (Fig. 5). Linear models must include all the grid points in this composite block in the FFT evaluation, whereas diagnostic models need only consider the grid points within the immediate region of interest. Hence a more appropriate metric is the total CPU time needed to obtain a solution, not the time per grid point. In any event, it appears from the literature that the times for both classes of models are on the order of a few minutes, and

perhaps an order of magnitude less, given today's chip speeds. This is well within the requirements for real-time applications. Issues of accuracy and ease of use should thus take precedence over speed.

Insofar as their applicability to NEST's mission, the biggest drawbacks of the idealized linear models considered in this section are the assumptions embodied in Eqs. (48) and (49). Any solution predicated on small-perturbation analysis is immediately suspect for flows involving phenomena such as stagnation points, separation, and recirculation, where by definition the perturbations are of the same magnitude as the flow about which the linearization is performed. Yet these very regions are among the most likely to accumulate lethal contaminants. Reliance on a linear model could thus lead to erroneous assessments in situations involving such phenomena.

Of course, there is no way to guarantee *a priori* that the results of a linear model will in fact satisfy Eq. (48), but certainly a necessary (though perhaps not sufficient) condition is that the terrain be gently sloping, as reflected in Eq. (49). Jackson and Hunt (1975) state that h/L less than ~ 0.05 should be sufficient to justify linearization for most purposes. Assuming a typical slope angle has a tangent of $h/(2L)$ (*cf.* Fig. 4), this implies inclinations of no more than ~ 2°. But it has been noted by several authors that such models are routinely applied to terrain slopes that lay outside this strict range of validity: Mason and King (1985) found good agreement with observations of flow speedup over hills with slopes of ~ 24°. Carruthers, *et al.* (1988) claim useful results for slopes of the order of 0.25 to as great as 0.5. Assuming here that by 'slope' they mean the tangent of the angle between the surface and the horizontal, *i.e.*, $h/(2L)$ in Fig. 4, this implies terrain inclinations in the range of 14°–27°. Finardi, *et al.* (1993) claim reasonably good results out to $h/L \leq 0.3$–0.4, or inclinations of 9°–11°. Of course, terms such as 'good' and 'useful' are themselves subjective, as is the choice of values for h and L when the terrain is complex. In any event, linear models are clearly inappropriate for use in mountainous regions, or wherever local features such as bluffs violate these assumptions.

It should also be noted that those linear models that purport to predict the influence of multiple mechanisms, *e.g.*, changes in surface elevation, roughness, and stratification, do so by assuming each mechanism acts independently of the others. That is, the effects of elevation changes are computed assuming uniform roughness and neutral stratification, while the effects of roughness changes are calculated for a level plain and neutral stratification, and so on. Then, because the underlying equations are linear, a composite flow field incorporating the effects of all the mechanisms is obtained by superposing (adding) the separate solutions (Walmsley, *et al.* (1986), Astrup, *et al.* (1997)). It must be recognized, however, that this neglects any nonlinear interactions between the mechanisms—an assumption borne out of the desire to be able to express the results analytically to the greatest extent possible. Hunt, *et al.* (1991) cite evidence that this may be valid for accelerating flows, but not where significant deceleration is present.

In addition to the numerous approximations and ambiguous choices of physical parameter values (*e.g.*, h and L) that a linear model forces on the user, there is also the question of how large to make the transition zone and uniform plain that are imagined to surround the region of interest (*cf.* Fig. 5). If L/L_R and L_T/L_R are too small, edge effects resulting from the artificially imposed periodicity will contaminate the results. On the other hand, values larger than needed will waste valuable computational time computing solutions at more grid points than necessary.

To the author's knowledge, this question has never been addressed systematically, and it represents a weak link in the arguments of such methods' proponents.

In light of these uncertainties, even when good agreement with observational data is demonstrated, there remains the nagging doubt that it could have been the result of a fortuitous self-cancellation of errors of opposite sign. J. C. R. Hunt is one of the originators of this type of model, and has probably co-authored more papers on the subject than anyone else. *Boundary-Layer Meteorology* published a brief question and answer exchange with the authors immediately following Hunt and Richards (1984) paper. In response to the question: "You have shown a few examples of linear solutions to flow over complex terrain. Could you please summarize common features to flows where linear theory works well? There are forced boundary flows which have a nice linear solution although [the] velocity perturbations are quite high." Hunt replied: "It is difficult to know exactly when the linear solutions for an air flow over hills are inaccurate. If the linear theory is used and large perturbations are calculated, then the results should be treated with caution... But in general it is hard to define the limitations of linear models without having made nonlinear calculations."

It seems reasonable to conclude then that linear models are best suited for more deliberative environments, such as air quality studies, predicting maximum wind loads on buildings, or evaluating alternative sites for wind turbines. Such applications afford the time to ponder and perhaps answer some of the questions raised above. However, NEST must make its hazard assessments in "real time", with little or no opportunity for second-guessing. It is concluded that at the present time there are too many open questions regarding the application of linearized models to complex terrain to recommend their use by NEST.

4. SUMMARY & CONCLUSIONS

This report has attempted to review the published literature on both *diagnostic* (*mass-consistent*) and *linearized* wind models from the perspective of the type of applications dealt with by Sandia's Nuclear Emergency Support Team (NEST). Diagnostic models adjust an initial (usually interpolated) wind field so as to satisfy the continuity equation at each grid point, and the boundary condition of no throughflow at the surface. Linear models, in addition to satisfying the continuity equation, also solve the equations representing conservation of momentum. As the latter include viscous terms, they are able to enforce the no-slip condition at the surface as well. Discussion has focussed on the theoretical background of each class, as well as the distinguishing characteristics, advantages, and disadvantages of the various models within each class.

The broad question is which of these classes of models—diagnostic or linear—lends itself most readily to emergency-response scenarios where "real-time" calculations are the order of the day. Linear models are concluded to be less suitable for use by NEST, despite the fact that they purport to include more physics (*i.e.*, the momentum equations) in their predictions. This is because the price paid for linearizing the normally nonlinear momentum equations is steep: the flow is everywhere assumed to be a small-perturbation about a single, unidirectional oncoming flow (*cf.* Eq. (48)-(49)). Their predictions are thus strictly valid only for very gently sloping terrain—slopes of no more than a few degrees (Jackson and Hunt (1975), Finardi, *et al.* (1993)). In practice, these models are routinely applied well outside their strict range of validity—to slopes as steep as 25°-30°— and may still yield qualitatively reasonable results (Mason and King (1985), Carruthers, *et al.* (1988), Finardi, *et al.* (1993)). Yet this must be regarded as fortuitous, due perhaps to the self-cancellation of compensating errors. Flows involving stagnation points, separation, and recirculation zones—as often occur on the leeward sides of hills and mountains, for example—by definition involve large perturbations from the oncoming flow, and so cannot be expected to be faithfully represented by such a model. Yet these are the very types of regions in which contaminants are likely to accumulate; reliance on such a model in these situations is problematic at best. That is not to say that a diagnostic model is guaranteed to accurately reflect such phenomena. But at least it has the hope of doing so, *provided representative observations are used to generate the interpolated field from which it starts*. More will be said on this point later.

In addition to the uncertainties introduced by an analysis predicated on very gently sloping terrain, there are other assumptions and ambiguities associated with linear theories that make their application to the real world somewhat problematic. For one, when dealing with complex terrain, how does one unambiguously set values for h and L (Fig. 4)? The turbulent Reynolds stresses in the inner region are approximated using a mixing length model, which represents them algebraically in terms of the mean velocity gradients; but it would be simplistic to think such a model will apply universally. Also, when multiple forcing mechanisms are present, *e.g.*, changes in surface elevation, roughness, and stratification, the linear models neglect any possible nonlinear interactions between them, and simply sum the effects of each mechanism acting independently of the others. Those models that include roughness variations and stratification effects may also require inputs regarding the spatial variations in z_0, and atmospheric stability, that (like those required for full Primitive Equation models) are not readily available. Finally, to the author's knowledge, no one has performed a systematic study

of the degree to which results are influenced by the artificially-introduced horizontal periodicity (Fig. 5), and the values chosen for the associated parameters L/L_R and L_T/L_R.

Related to the issue of accuracy, a further perceived disadvantage of the linear theories, is that, because they linearize about a single oncoming flow, it is not clear how wind observations from multiple stations (if available) can be assimilated into the results. Hunt, *et al.* (1991) point out the need for further research on this topic. Astrup, *et al.* (2001) (p. 106) mention an approach for doing so that involves weighted averages of multiple LINCOM-predicted flowfields, but the description is very brief and rather cryptic.

Investigations comparing the predictions of diagnostic and linear models are few and far between (*e.g.*, Walmsley, *et al.* (1990) and Finardi, *et al.* (1993)). Most have been performed by the developer(s) of one or more of the models being considered, raising questions about their impartiality. An important exception in this regard is the investigation by Finardi, *et al.* (1993), which compared predictions from two diagnostic (MATHEW and MINERVE) and two linear (MS3DJH/3R and FLOWSTAR III) models against two-dimensional wind tunnel data for neutrally-stable flow. None of the investigators had been involved in the development of the models. Unfortunately, the published results use different metrics to assess the fidelity of the diagnostic and linear models. Hence, the focus was primarily on contrasting MS3DJH/3R *vs*. FLOWSTAR, and MATHEW *vs*. MINERVE, and less so on comparing linear *vs*. diagnostic models. Nevertheless, for applications to complex terrain, the authors give an implicit nod to the diagnostic models when they conclude that (italics added by present author for emphasis): i) "… linearized models are a powerful tool for dealing with flow over *simple* topography when only the oncoming wind profile is given"; and ii) "the ability of mass-consistent models to describe the main features of a wind field over *complex* terrain depends on the availability of properly sited input data. To attain a satisfactory description, every main flow feature has to be depicted by some input wind profile".

In summary, while linear models may provide flow fields that incorporate both mass and momentum conservation in a very idealized sense, their accuracy when applied to steep, rapidly-changing terrain is debatable. These issues can only be addressed in hindsight through observation, or as noted in the Q&A immediately following Hunt and Richards (1984), by comparison with more complex nonlinear calculations. For these reasons, it is felt that linear models are best suited for more deliberative environments, such as air quality studies, predicting maximum wind loads on buildings, or evaluating alternative sites for wind turbines. Such applications afford the time to ponder and perhaps answer some of the questions raised above. However, NEST must make its hazard assessments in "real time", with little or no opportunity for second-guessing, an environment that linear models do not lend themselves to. Nevertheless, it is recommended that the team keep abreast of developments in this class of models, particularly if a means of linearizing the equations is found that does not restrict their applicability to gently sloping terrain. Extensions such as the inclusion of the energy equation in the system (Troen and de Baas (1986)) are particularly intriguing.

It is thus concluded that use of a diagnostic model to correct the interpolated field represents the next logical step up in wind modeling for the NEST group. This will eliminate any sources and sinks from the flow by enforcing Eq. (1), and assure that the wind goes around or over obstacles—rather than through them!—by enforcing the no-throughflow boundary condition at

the surface. These models assume only that the flow is incompressible, typically require only a few minutes of computer time, and require a minimal number of subjective inputs by the user. Furthermore, they can easily accommodate an arbitrary number of wind observations, as reflected by the initial interpolated field.

The next question is then: do any of the four approaches to diagnostic modeling, as outlined in Table 1 on p. 4, clearly stand out as superior to the others? The Direct-Differencing approach (§2.1) is overly simplistic in that it neglects any errors in u_i and v_i, and places the entire burden of satisfying Eq. (1) on the vertical component alone. Unless u_i and v_i are known very accurately, it is prone to predict unreasonably large magnitudes for w that make it inappropriate for use in stable conditions, where one expects w to be of very small magnitude. Point-Iterative schemes (§2.2) are in a sense the converse of Direct-Differencing, in that they assume the vertical component is negligible, and adjust only u and v to cancel any initial divergence. Models in this category are not suited for unstable conditions. As its name suggests, the Hybrid approach (§2.3) is a combination of the first two which attempts to spread responsibility for satisfying Eq. (1) across all three wind components, and hopefully prove applicable under a broader spectrum of conditions. But it suffers from too many *ad hoc* assumptions and approximations, not to mention lapses in specificity. There remains a good deal of subjectivity in applying this approach to new terrain for which a model has yet to be "tuned".

The only category of diagnostic model that treats the three wind components simultaneously in a unified framework, and with the least ambiguity, is the Variational Calculus approach (§2.4) first articulated by Sasaki (1958, 1970a,b). It is also the approach that has attracted the greatest following, as evidenced by the number of different models that are based on this formulation. Significantly, the excellent review of mass-consistent models presented by Ratto, *et al.* (1994) considered only models in the Variational Calculus category. The ambiguities[†] unique to this approach are: 1) whether to assign α_1 and α_2 constant values, or allow them to vary independently in space; and 2) how these Gauss precision moduli (also known as weighting factors, or transmissivity coefficients) can be related to atmospheric stability. More data are needed, and much work remains to be done, on the question of whether a universal parameterization of $\alpha^2(St)$, or $\alpha^2(Fr)$, can be developed that covers the gamut from stable to neutral to unstable conditions. A possible drawback to this approach is the need to use an iterative scheme to solve Eq. (33) or (37), with the attendant questions of convergence and robustness such a technique entails. The large community of users suggests this is not a significant problem, and reported run times on the order of a few minutes are well within the bounds of what is required of "real-time" models. It is therefore concluded that a model based on the Variational Calculus approach is best suited for use by NEST.

Of the models in this category, MATHEW (Sherman, (1978)) and MINERVE (Geai (1987a,b)) appear to have been used the most extensively. As noted earlier, Finardi, *et al.* (1993) compared their predictions against wind tunnel data for neutrally-stratified flow over isolated, two-dimensional hills of variable slope. Neither model was able to adequately describe the wind field using only one or two vertical wind profiles to generate the initial

[†]There are other ambiguities, such as: the horizontal extent of the domain, where to place the top, what size grid cell to use, which interpolation scheme, *etc*. But these are always present, regardless of which approach to diagnostic modeling one follows. The intent here is to focus on only those that are unique to a given category.

interpolated field. However, when three profiles were used, several of the flows were well depicted by either model everywhere but in the wake region. In this regard, it cannot be emphasized enough that, in addition to satisfying Eq. (1), these models also minimize the difference between the adjusted and interpolated wind fields. Thus, *any phenomena* (such as, in this case separation and recirculation on the leeward side of obstacles) *not reflected in the initial observations will not be depicted in the adjusted wind field*, as has been noted repeatedly in the literature (*e.g.*, Moussiopoulos, *et al.* (1988), Ross, *et al.* (1988), Boughton and DeLaurentis (1992), Finardi, *et al.* (1993), Ratto, *et al.* (1994), and Banta, *et al.* (1996).

Overall, Finardi, *et al.* (1993) found that MINERVE did a much better job than MATHEW at predicting *w*. They ascribe most of the differences between results generated by the two models to the fact that MINERVE uses the more accurate terrain-following coordinate (TFC) approach to represent the terrain variations, as opposed to the stair-step terrain (SST) representation used by MATHEW. The latter makes it more difficult to accurately satisfy the surface boundary condition unless a very fine grid is used, which leads to prohibitive run times. The use of TFC in MINERVE permits both a more accurate enforcement of the surface condition, and the use of variable grid cell sizes in the vertical direction. This allows more efficient use of computing resources, because grid points can be clustered near the surface, where gradients are strongest, and spaced further apart near the top of the domain, where they are likely to be weakest. The authors point out that how well any such model does depends strongly on not only the quality and quantity of the observational data, but on choosing an appropriate value of α as well. They found that high values of α (> 1) seemed to give the best agreement, which corresponds to leaving the horizontal wind field virtually unchanged. They question (pp. 286-287) the utility of attempts to functionally relate α to atmospheric stability criteria (*e.g.*, Ross, *et al.* (1988, 1991) and Moussiopoulos, *et al.* (1988)), but don't offer any concrete suggestions as to how else α might be set on an objective, *a priori* basis.

While Finardi, *et al.* (1993) avoid making any conclusive statements as to whether they found MATHEW or MINERVE preferable, it is interesting to note that in two subsequent investigations that Finardi participated in, MINERVE was chosen for further study while MATHEW was not. At the least, it seems reasonable to interpret this as a tacit endorsement of MINERVE over MATHEW. Finardi, *et al.* (1998) successfully used it to model wind variations at a site in the Appennini mountains in central Italy being considered for wind turbine installation. Its predictions were comparable to those obtained from application of the RAMS prognostic model. Desiato, *et al.* (1998) applied both MINERVE and CONDOR to reconstruct the 3D wind fields during the TRANSALP-89 meteorological and tracer experiment conducted in the Swiss Alps. Though each used a different numerical solution technique, given the same input data and values for α, both models produced approximately the same solution, thus providing a cross-check on their validity.

MINERVE has been subjected to numerous and detailed evaluations/validations since its initial development. Further, the model has been tested by a number of independent organizations (Bradley, *et al.* (1997), Cox, *et al.* (1998)) not associated with its original developers, the French Electricity Board (Geai, (1987a,b)). This is viewed as a favorable indicator of both its accuracy, and its ease of use. The list of organizations includes: the Italian Electricity Board (ENEL) (Finardi, *et al.* (1993,1998), Desiato, *et al.* (1998), Morselli, *et al.* (1997)); the Swiss Radio Protection Board; Science Applications International Corporation

(SAIC) (Sontowski, *et al.* (1995), Sontowski and Dougherty (1996), Cox, *et al.* (1998)); the Defense Threat Reduction Agency (DTRA) and its predecessors DNA and DSWA (Bradley, *et al.* (1997)); Software Solutions and Environmental Services Company (SSESCO) (*cf.* **http://www.ssesco.com/RITE.html**); and ARIA Technologies (France) (*cf.* **http://www.airparif.asso.fr/english/modelisation/simpar.htm**). The above investigations include comparisons with wind tunnel data for flow over idealized shapes, as well as atmospheric flows in both North America and Europe, including the Appalachian mountains, the Swiss Alps, the DOE Hanford site, and White Sands Missile Range.

Some evaluations systematically withheld selected wind data measurements from the observed/interpolated wind field used as input to MINERVE. The adjusted wind field was then compared against the withheld data to gauge the effectiveness of the model. MINERVE was found to give good to excellent results, depending on the number and location of observations used as input. Finardi, *et al.* (1993) found that predictions with as few as two ground measurements and one vertical profile were "encouraging" for practical applications. Bradley, *et al.* (1997) and Cox, *et al.* (1998) are a bit more conservative, and conclude that for satisfactory results a minimum of three surface observations and one upper-air profile are needed. Generally speaking, the more observations the better, since as noted earlier, any local phenomena not reflected in the interpolated field will likely not be present in the adjusted field. However, Desiato, *et al.* (1998) caution that more observations do not necessarily improve the accuracy of the results. They argue that the input data should only reflect phenomena of a scale that is resolvable by the grid being used. Very localized flow phenomena caused by small topographic features that are below the scale of the grid will be spatially expanded by the interpolation process, and hence should be avoided in the observed dataset. Similarly, as the interpolation normally depends only on the horizontal distance between the observation station and a grid point, the effect of any topographic barrier between them is not taken into account, which can lead to peculiar results. In such instances, they suggest using paired observations, one on either side of the barrier, to counterbalance this effect.

MINERVE has several different interpolation schemes available for generating the initial field from the observations, including one employing inverse distance-squared weighting (the scheme currently used in ERAD (Boughton and DeLaurentis (1992)) and AIRRAD (Sagartz (1997)). The choice of which to use can be made based on the nature or distribution of the observed data. The relative amount of adjustment made to the vertical and horizontal wind components is determined by the Gauss precision moduli, α_1 and α_2. Calculations typically assume a constant value for $\alpha = \alpha_1/\alpha_2$, as in Eq. (37); or, the model can also allow the Gauss precision moduli α_1 and α_2 to vary spatially in three dimensions (Eq. (33)). Values for these weight factors may either be specified by the user, or calculated internally by the code (Cox, *et al.* (1998)). If calculated internally, the weight factors are computed in terms of some measure of atmospheric stability, typically depending on the vertical temperature profile. Various parameterizations of α^2 in terms of stability are available in the model (Sontowski and Dougherty (1996)), including the $\alpha^2(St)$ relation in Eq. (43), proposed by Moussiopoulos, *et al.* (1988). Alternatively, if α_1 and α_2 are not related to atmospheric stability, they could possibly be used to enforce other conditions on the adjusted wind field. For example, if α_1 and α_2 are given very high values at grid points in the immediate vicinity of the observed data and low values elsewhere, the adjusted field should be very close to the initial field (and hence the observations) at those points, with more latitude to adjust away from them. It is not known

whether such a specification might introduce convergence difficulties, however. Recall also that Liu and Goodin (1976) felt that the high-frequency contamination of their Point-Iterative scheme's predictions (p. 13) was the result of too strict an adherence to the observed data points.

NEST may be called upon to make hazard assessments in situations where only a single surface observation, or perhaps none, is available. In light of the minimum input requirements described above, in such situations will the use of MINERVE, or any diagnostic model for that matter, represent added value to the transport and diffusion calculations? To the extent that they would otherwise be forced to rely on a uniform wind vector equal to the one observed (or worse, assumed) value, the answer is yes. Yes, because the model will adjust the wind to go around and over those terrain features that are resolvable by the finite-difference grid, rather than through them, and it will do so without introducing any spurious sources or sinks in the flow interior. However, effects such as land/sea breezes, or separation and recirculation on the leeward side of obstacles, would not be represented, as they would not be present (under the stated assumptions) in the observations. The extent to which this will influence the final concentration predictions is another matter, and will no doubt vary from case to case.

Accordingly, it is recommended that as a first step in developing a diagnostic modeling capability, the Sandia NEST group explore the possibility of licensing the MINERVE software from Science Applications International Corporation (SAIC), who licenses MINERVE in the United States, and continues to do further development work on it. This is likely to be much more cost-effective than developing a new code "from scratch" in-house. Furthermore, much of the work that would have had to be devoted to validating a new model has already been performed, and the large community of users represents a base of experience that the team can draw upon. Presumably, SAIC would also be willing to provide technical support and training in its use.

Finally, it should be remembered that the predictions of the various models discussed here will likely be influenced almost as much by the skill level and experience of the user, as by the choice of model. That is why we have tried to focus on those models which are the least arbitrary to apply. But *some* ambiguity is the price one must pay for attempting to pin down a three-dimensional vector field based on only the single scalar equation, Eq. (1). The problem is simply under-determined, and therefore a completely objective solution is by definition impossible.

REFERENCES ON DIAGNOSTIC MODELS

Allwine, K. J., Dabberdt, W. F. and Simmons, L. L. (1998) *Peer Review of the CALMET/ CALPUFF Modeling System*, EPA Contract No. 68-D-98-092, compiled and submitted by the KEVRIC Company, Inc., Durham, NC.

Anderson, G. E. (1971) "Mesoscale Influences on Wind Fields," *Journal of Applied Meteorology,* Vol. 10, pp. 377-386.

Banta, R. M., Olivier, L. D., Gudiksen, P. H. and Lange, R. (1996) "Implications of Small-Scale Flow Features to Modeling Dispersion over Complex Terrain," *Journal of Applied Meteorology,* Vol. 35, pp. 330-342.

Barna, M. and Lamb, B. (2000a) "Improving Ozone Modeling in Regions of Complex Terrain Using Observational Nudging in a Prognostic Meteorological Model," Atmospheric Environment, Vol. 34, pp. 4889-4906.

Barna, M., Lamb, B., O'Neill, S., Westberg, H., Figeroa-Kaminsky, C., Otterson, S., Bowman, C. and DeMay, J. (2000b) "Modeling Ozone Formation and Transport in the Cascadia Region of the Pacific Northwest," *Journal of Applied Meteorology,* Vol. 39, pp. 349-366.

Barnard, J. C., Wegley, H. L. and Hiester, T. R. (1987) "Improving the Performance of Mass-Consistent Numerical Models Using Optimization Techniques," *Journal of Climate and Applied Meteorology,* Vol. 26, pp. 675-686.

Bhumralkar, C. M., Mancuso, R. L., Ludwig, F. L. and Renné, D. S. (1980) "A Practical and Economic Method for Estimating Wind Characteristics at Potential Wind Energy Conversion Sites," *Solar Energy,* Vol. 25, No. 1, pp. 55-65.

Boughton, B. A. and DeLaurentis, J. M. (1992) *Description and Validation of ERAD: An Atmospheric Dispersion Model for High Explosive Detonations,* Sandia National Laboratories Report SAND92–2069, Albuquerque, New Mexico.

Bradley, S., Mazzola, T., Ross, R., Srinivasa, D., Fry, R., Bacon, D., McGahan, J., Bauer, B., Newall, R., Sontowski, J., Sykes, I., Sjoreen, A., Morris, R. and Worley, B. (1997) *Initial Verification and Validation of HPAC 1.3,* Technical Report DSWA-TR-96-88, prepared by Logicon R&D Associates, Alexandria, VA, for the Defense Special Weapons Agency.

Canneill, J.-Y., Geai, P., Perdriel, S. and Biscay, P. (1990) "Assessing the Dispersion of Radioactive Effluents at Regional Scale: the HERMES and MINERVE Codes," in the *Proceedings of the 2nd International Workshop on Real-Time Computing of the Environmental Consequences of an Accidental Release to the Atmosphere from a Nuclear Installation*, held in Luxembourg, May 16-19, 1989, pp. 371-402.

Carmichael, G. R. and Peters, L. K. (1980) "The Transport, Chemical Transformation and Removal of SO_2 and Sulfate in the Eastern United States," *Atmospheric Pollution 1980*, Proceedings of the 14th International Colloquium, Paris, France, May 5-8, 1980, edited by Benarie, M. M., *Studies in Environmental Science*, Vol. 8, pp. 31-36.

Chen, J., Bornstein, R. and Lindsey, C. G. (1999) "Transport of a Power Plant Tracer Plume over Grand Canyon National Park," *Journal of Applied Meteorology*, Vol. 38, pp. 1049-1068.

Courant, R. and Hilbert, D. (1953) *Methods of Mathematical Physics, Vol. 1*, Interscience Publishers, New York, NY, 561 pp.

Cox, R. M., Sontowski, J., Fry Jr., R. N., Dougherty, C. M. and Smith, T. J. (1998) "Wind and Diffusion Modeling for Complex Terrain," *Journal of Applied Meteorology*, Vol. 37, pp. 996-1009.

Danard, M. (1977) "A Simple Model for Mesoscale Effects of Topography on Surface Winds," *Monthly Weather Review*, Vol. 105, No. 5, pp. 572-581.

Davis, C. G., Bunker, S. S. and Mutschlecner, J. P. (1984) "Atmospheric Transport Models for Complex Terrain," *Journal of Climate and Applied Meteorology*, Vol. 23, pp. 235-238.

Desiato, F., Finardi, S., Brusasca, G. and Morselli, M. G. (1998) "TRANSALP 1989 Experimental Campaign—I. Simulation of 3D Flow with Diagnostic Wind Field Models," *Atmospheric Environment*, Vol. 32, No. 7, pp. 1141-1156.

Dickerson, M. H. (1978) "MASCON—A Mass Consistent Atmospheric Flux Model for Regions with Complex Terrain," *Journal of Applied Meteorology*, Vol. 17, No. 3, pp. 241-253.

Douglas, S. G. and Kessler, R. C. (1991) "Analysis of Mesoscale Airflow Patterns in the South-Central Coast Air Basin during the SCCCAMP 1985 Intensive Measurement Periods," *Journal of Applied Meteorology*, Vol. 30, No. 5, pp. 607-631.

Ehrendorfer, M., Hantel, M. and Wang, Y. (1994) "A Variational Modification Algorithm for Three-Dimensional Mass Flux Non-Divergence," *Quarterly Journal of the Royal Meteorological Society*, Vol. 120, pp. 655-698.

Endlich, R. M. (1967) "An Iterative Method for Altering the Kinematic Properties of Wind Fields," *Journal of Applied Meteorology*, Vol. 6, pp. 837-844.

Endlich, R. M., Ludwig, F. L., Bhumralkar, C. M. and Estoque, M. A. (1982) "A Diagnostic Model for Estimating Winds at Potential Sites for Wind Turbines," *Journal of Applied Meteorology*, Vol. 21, No. 10, pp. 1441-1454.

Endlich, R. M. (1984) "Wind Energy Estimates by Use of a Diagnostic Model," *Boundary-Layer Meteorology*, Vol. 30, pp. 375-386.

Finardi, S., Brusasca, G., Morselli, M. G., Trombetti, F. and Tampieri, F. (1993) "Boundary-Layer Flow over Analytical Two-Dimensional Hills: A Systematic Comparison of Different Models with Wind Tunnel Data," *Boundary-Layer Meteorology*, Vol. 63, No. 3, pp. 259-291.

Finardi, S., Morselli, M. G., Brusasca, G. and Tinarelli, G. (1997) "A 2-D Meteorological Pre-Processor for Real-Time 3-D ATD Models," *International Journal of Environment and Pollution*, Vol. 8, Nos. 3-6, pp. 478-488.

Finardi, S., Tinarelli, G., Faggian, P. and Brusasca, G. (1998) “Evaluation of Different Wind Field Modeling Techniques for Wind Energy Applications over Complex Topography,” *Journal of Wind Energy and Industrial Aerodynamics*, Vol. 74-76, pp. 283-294.

Forsythe, G. E. and Wasow, W. R (1960) *Finite-Difference Methods for Partial Differential Equations*, Wiley, 444 pp.

Fox, D. G. “Judging Air Quality Model Performance,” *Bulletin of the American Meteorological Society*, Vol. 62, No. 5, pp. 599-609.

Gallino, S., Mazzino, A. and Ratto, C. F. (1998) “A Simple Procedure to Account for Non-Kinematic Effects in a Mass-Consistent Wind Model,” *Journal of Wind Energy and Industrial Aerodynamics*, Vol. 74-76, pp. 229-237.

Geai, P. (1987a) *Reconstitution Tridimensionelle d’un Champ de Vent dans un Domaine á Topographie Complexe á Partir de Measures in situ*, Final Report DER/HE/34-87.05, Electricité de France, Chatou, France.

Geai, P. (1987b) *Methode D’Interpolation et de Reconstitution Tridimensionelle d’un Champ de Vent: Le code d’analyse objective MINERVE*, Report ARD-AID: E34-E11, Electricité de France, Chatou, France, 177 pp.

Gelbard, F. (1999) *Current Status on Wind Field Modeling for Chem/Bio/Nuc Hazard Dispersal*, Sandia National Laboratories, Albuquerque NM.

Giarola, S., Grippa, G. and Meneguzzo, F. (1995) “DI.M.C.OR: A Software Package for Diagnostic Wind Reconstruction,” *Environmental Software*, Vol. 10, No. 2, pp. 129-136.

Givati, R., Flocchini, R. G., and Cahill, T. A. (1996) “Modeling Sulfur Dioxide Concentrations in Mt. Rainier Area during PREVENT,” Atmospheric Environment, Vol. 30, No. 2, pp. 255-267.

Godfrey, J. J. and Clarkson, T. S. (1998) “Air Quality Modeling in a Stable Polar Environment—Ross Island, Antarctica,” *Atmospheric Environment*, Vol. 32, No. 17, pp. 2899-2911.

Goodin, W. R., McRae, G. J. and Seinfeld, J. H. (1979) “A Comparison of Interpolation Methods for Sparse Data: Application to Wind and Concentration Fields,” *Journal of Applied Meteorology*, Vol. 18, pp. 761-771.

Goodin, W. R., McRae, G. J. and Seinfeld, J. H. (1980) “An Objective Analysis Technique for Constructing Three-Dimensional Urban-Scale Wind Fields,” *Journal of Applied Meteorology*, Vol. 19, pp. 98-108.

Grell, G. A., Dudhia, J. and Stauffer, D. R. (1994) *A Description of the Fifth-Generation Penn State/NCAR Mesoscale Model (MM5)*, NCAR Technical Note NCAR/TN-398+STR, National Center for Atmospheric Research, Boulder, CO.

Gross, G. (1996) “On the Applicability of Numerical Mass-Consistent Wind Field Models,” *Boundary-Layer Meteorology*, Vol. 77, pp. 379-394.

Guo, X. and Palutikof, J. P. (1990) “A Study of Two Mass-Consistent Models: Problems and Possible Solutions,” *Boundary-Layer Meteorology*, Vol. 53, pp. 303-332.

Harada, M., Hayashi, S. and Wakimizu, K. (2000) “Introduction of a Genetic Algorithm to a Mass-Consistent Model,” *Journal of the Faculty of Agriculture, Kyushu University*, Vol. 44, No. 3-4, pp. 403-418.

Hunt, J. C. R. and Snyder, W. H. (1980) “Experiments on Stably and Neutrally Stratified Flow Over a Model Three-Dimensional Hill,” *Journal of Fluid Mechanics*, Vol. 96, pp. 671-704.

Ishikawa, H. (1991) “Development of Regionally Extended/Worldwide Version of System for Prediction of Environmental Emergency Dose Information: WSPEEDI, (I) Application of Mass-Consistent Wind Field Model to Synoptic Wind Fields,” *Journal of Nuclear Science and Technology*, Vol. 28, No. 6, pp. 535-546.

Ishikawa, H. (1994) “Mass-Consistent Wind Model as a Meteorological Preprocessor for Tracer Transport Models,” *Journal of Applied Meteorology*, Vol. 33, No. 6, pp. 733-743.

Kaplan, H. and Dinar, N. (1996) “A Lagrangian Dispersion Model for Calculating Concentration Distribution within a Built-Up Domain,” *Atmospheric Environment*, Vol. 30, No. 24, pp. 4197-4207.

Kim, J. Y., Ghim, Y. S., Kim, Y. P. and Dabdub, D. (2000) “Determination of Domain for Diagnostic Wind Field Estimation in Korea,” *Atmospheric Environment*, Vol. 34, pp. 545-601.

King, D. S. and Bunker, S. B. (1984) “Application of Atmospheric Transport Models for Complex Terrain,” *Journal of Climate and Applied Meteorology*, Vol. 23, pp. 239-246.

Kitada, T., Kaki, A., Ueda, H. and Peters, L. K. (1983) “Estimation of Vertical Air Motion from Limited Horizontal Wind Data—A Numerical Experiment,” *Atmospheric Environment*, Vol. 17, No. 11, pp. 2181-2192.

Kumar, N. and Russell, A. G. (1996) “Comparing Prognostic and Diagnostic Meteorological Fields and Their Impacts on Photochemical Air Quality Modeling,” *Atmospheric Environment*, Vol. 30, No. 12, pp. 1989-2010.

Kunz, R. and Moussiopoulos, N. (1997) “Implementation and Assessment of a One-Way Nesting Technique for High-Resolution Wind Flow Simulations,” *Atmospheric Environment*, Vol. 31, No. 19, pp. 3167-3176.

Lamprecht, R. and Berlowitz, D. (1998) “Evaluation of Diagnostic and Prognostic Flow Fields over Prealpine Complex Terrain by Comparison of the Lagrangian Predictions of Concentrations with Tracer Measurements,” *Atmospheric Environment*, Vol. 32, No. 7, pp. 1283-1300.

Lange, R. (1978) “ADPIC—A Three-Dimensional Particle-in-Cell Model for the Dispersal of Atmospheric Pollutants and its Comparison to Regional Tracer Studies,” *Journal of Applied Meteorology*, Vol. 17, pp. 320-329 (companion paper to Sherman, C. (1978)).

Liu, C. Y. and Goodin, W. R., (1976), "An Iterative Algorithm for Objective Wind Field Analysis," *Monthly Weather Review*, Vol. 104, pp. 784-792.

Liu, M.-K. and Yocke, M. A. (1980) "Siting of Wind Turbine Generators in Complex Terrain," Journal of Energy, Vol. 4, *Journal of Energy*, pp. 10-16.

Ludwig, F. L. and Byrd, G. (1980) "An Efficient Method for Deriving Mass-Consistent Flow Fields from Wind Observations in Rough Terrain," *Atmospheric Environment*, Vol. 14, pp. 585-587.

Ludwig, F. L., Livingston, J. M. and Endlich, R. M. (1991) "Use of Mass Conservation and Critical Dividing Streamline Concepts for Efficient Objective Analysis of Winds in Complex Terrain," *Journal of Applied Meteorology*, Vol. 30, pp. 1490-1499.

Martens, R., Thielen, H., Sperling, T. and Maβmeyer, K. (2000) "Validation of a Mass Consistent Flow Model as Part of a Decision Support System," *International Journal of Environment and Pollution*, Vol. 14, No. 1-6, pp. 573-580.

Mass, C. F. and Dempsey, D. P. (1985) "A One-Level Mesoscale Model for Diagnosing Surface Winds in Mountainous and Coastal Regions," *Monthly Weather Review*, Vol. 113, No. 7, pp. 1211-1227.

Mathur, R. and Peters, L. K. (1990) "Adjustment of Wind Fields for Application in Air Pollution Modeling," *Atmospheric Environment*, Vol. 24A, No. 5, pp. 1095-1106.

Melas, D., Zionas, I. and Kioutsioukis, I. (1998) "Real Time Calculation of the Dispersion of Air Pollutants from Industrial Stacks Using a Personal Computer," *Fresenius Environmental Bulletin*, Vol. 7, No. 3-4, pp. 134-140.

Melas, D., Abbate, G., Haralampopoulos, D. and Kelesidis, A. (2000) "Estimation of Meteorological Parameters for Air Quality Management: Coupling of Sodar Data with Simple Numerical Models," *Journal of Applied Meteorology*, Vol. 39, pp. 509-515.

Montero, G., Montenegro, R. and Escobar, J. M. (1998) "A 3-D Diagnostic Model for Wind Field Adjustment," *Journal of Wind Energy and Industrial Aerodynamics*, Vol. 74-76, pp. 249-261.

Montero, G. and Sanin, N. (2001) "3-D Modeling of Wind Field Adjustment Using Finite Differences in a Terrain Conformal Coordinate System," *Journal of Wind Energy and Industrial Aerodynamics*, Vol. 89, No. 5, pp. 471-488.

Morselli, M. G., Calori, G., Finardi, S. and Mazzola, C. (1997) "A 3-D Wind and Temperature Pre-Processor for ATD Models," International Journal of Environment and Pollution, Vol. 8, Nos. 3-6, pp. 489-499.

Moussiopoulos, N. and Flassak, Th. (1986) "Two Vectorized Algorithms for the Effective Calculation of Mass-Consistent Flow Fields," *Journal of Climate and Applied Meteorology*, Vol. 25, No. 6, pp. 847-857.

Moussiopoulos, N., Flassak, Th. and Knittel, G. (1988) "A Refined Diagnostic Wind Model," *Environmental Software*, Vol. 3, No. 2, pp. 85-94.

Pai, P., Farber, R. J., Karamchandani, P. and Tombach, I. (2000) "Assessment of the Nested Grid Model Estimates for Driving Regional Visibility Models in the Southwestern United States," *Journal of the Air & Waste Management Association*, Vol. 50, pp. 818-825.

Palomino, L. and Martín, F. (1995) "A Simple Method for Spatial Interpolation of the Wind in Complex Terrain," *Journal of Applied Meteorology,* Vol. 34, No. 7, pp. 1678-1693.

Panofsky, H. A and Dutton, J. A. (1984) *Atmospheric Turbulence—Models and Methods for Engineering Applications*, John Wiley & Sons, 397 pp.

Peaceman, D. W. and Rachford Jr., H. H. (1955) "The Numerical Solution of Parabolic and Elliptic Differential Equations," *Journal of the Society for Industrial and Applied Mathematics*, Vol. 3, pp. 28-41.

Pechinger, U., Langer, M., Baumann, K. and Petz, E. (2001) "The Austrian Emergency Response Modeling System TAMOS," *Physics and Chemistry of the Earth, Part B: Hydrology, Oceans, and Atmosphere*, Vol. 26, No. 2, pp. 99-103.

Pepper, D. W., Carrington, D. B. and Lombardo, J. M. (1998) "A Parallel h-Adaptive Finite Element Model for Atmospheric Transport Prediction," *Advances in Engineering Software*, Vol. 29, No. 3-6, pp. 359-363.

Peters, L. K., and Jouvanis, A. A. (1979) "Numerical Simulation of the Transport and Chemistry of CH_4 and CO in the Troposphere," *Atmospheric Environment*, Vol. 13, pp. 1443-1462.

Prabha, T. V. and Mursch-Radlgruber, E. (1999) "Investigation of Air-Pollution Distribution in Linz: Case Studies to Evaluate a K-Type Diffusion Model Coupled with a Mass-Consistent Wind Model," *Atmospheric Environment*, Vol. 33, pp. 4067-4080.

Ratto, C. F., Festa, R., Romeo, C., Frumento, O. A. and Galluzzi, M. (1994) "Mass-Consistent Models for Wind FIelds over Complex Terrain: The State of the Art," *Environmental Software*, Vol. 9, No. 4, pp. 247-268.

Reynolds, S. D., Roth, P. M. and Seinfeld, J. H. (1973) "Mathematical Modeling of Photochemical Air Pollution—I," *Atmospheric Environment*, Vol. 7, pp. 1033-1061.

Ross, D. G., Smith, I. N., Manins, P. C. and Fox, D. G. (1988) "Diagnostic Wind Field Modeling for Complex Terrain: Model Development and Testing," *Journal of Applied Meteorology,* Vol. 27, pp. 785-796.

Ross, D. G. and Fox, D. G. (1991) "Evaluation of an Air Pollution Analysis System for Complex Terrain," *Journal of Applied Meteorology,* Vol. 30, No. 7, pp. 909-923.

Ross, D. G. and Smith, I. N. (1991) "Discussion of 'Adjustment of Wind Fields for Application in Air Pollution Modeling' (by Mathur and Peters)," *Atmospheric Environment*, Vol. 25A, No. 10, pp. 2425-2427.

Sagartz, M. J. (1997) *Testing of the AIRRAD Fallout Prediction Code*, Sandia National Laboratories Report SAND97–2613, Albuquerque, New Mexico.

Sasaki, Y. (1958) "An Objective Analysis Based on the Variational Method," *Journal of the Meteorological Society of Japan*, Vol. 36, No. 3, pp. 77-88.

Sasaki, Y. (1970a) "Numerical Variational Analysis Formulated Under the Constraints as Determined by Longwave Equations and a Low-Pass Filter," *Monthly Weather Review*, Vol. 98, No. 12, pp. 884-898.

Sasaki, Y. (1970b) "Some Basic Formalisms in Numerical Weather Analysis," *Monthly Weather Review*, Vol. 98, No. 12, pp. 875-883.

Schecter, R. S. (1967) *The Variational Method in Engineering*, McGraw-Hill, New York, NY, 287 pp.

Scire, J. S., Robe, F. R., Fernau, M. E. and Yamartino, R. J. (2000) *A User's Guide for the CALMET Meteorological Model (Version 5)*, Earth Tech, Inc., Concord, MA. Available for download at URL: http://src.com/calpuff/calpuff1.htm

Sherman, C. A. (1978) "A Mass-Consistent Model for Wind Fields over Complex Terrain," *Journal of Applied Meteorology*, Vol. 17, pp. 312-319.

Sontowski, J., Cox, R. M., Dougherty, C. M. and Fry Jr., R. N. (1995) "Validation of a Mass Consistency Wind Model at White Sands Missile Range," *Proceedings of the 1995 Battlefield Atmospheric Conference*, White Sands Missile Range, NM, sponsored by U. S. Army Research Laboratory, pp. 64-76.

Sontowski, J. and Dougherty, C., (1996) *Multiscale Environmental Dispersion Over Complex Terrain—the MEDOC Models*, Technical Report DNA-TR-94-182, prepared for the Defense Nuclear Agency by Science Applications International Corporation, Wayne, PA.

Souto, J. A., Perez-Muñuzuri, V., deCastro, M., Souto, M. J., Casares, J. J. and Lucas, T. (1998), "Forecasting and Diagnostic Analysis of Plume Transport around a Power Plant," *Journal of Applied Meteorology*, Vol. 37, No. 10, pp. 1068-1083.

Stephens, J. J. (1967) "On Convergence of the Endlich Iteration Method," *Journal of Applied Meteorology*, Vol. 6, pp. 845-847.

Stohl, A., Baumann, K., Wotawa, G., Langer, M., Neininger, B., Piringer, M. and Formayer, H. (1997), "Diagnostic Downscaling of Large-Scale Wind Fields to Compute Local-Scale Trajectories," *Journal of Applied Meteorology*, Vol. 36, No. 7, pp. 931-942.

Strimaitis, D. G., Moore, G. E. and Douglas, S. G. (1991), "Analysis of Tracer Data Collected during the SCCAMP 1985 Intensive Measurement Periods," *Journal of Applied Meteorology*, Vol. 30, No. 5, pp. 674-706.

Sullivan, T. J., Ellis, J. S., Foster, C. S., Foster, K. T., Baskett, R. L., Nasstrom, J. S. and Schalk III, W. W. (1993) "Atmospheric Release Advisory Capability: Real-Time Modeling of

Airborne Hazardous Materials," *Bulletin of the American Meteorological Society*, Vol. 74, No. 12, pp. 2343-2361.

Thunis, P. and Bornstein, R. (1996) "Hierarchy of Mesoscale Flow Assumptions and Equations," *Journal of the Atmospheric Sciences*, Vol. 53, No. 3, pp. 380-397.

Tombrou, M., Bossioli, E. and Lalas, D. (1998) "An Application of a Simple Monte Carlo Dispersion Model in Complex Terrain," *Environmental Modeling & Software*, Vol. 13, pp. 45-58.

Traci, R. M., Phillips, G. T. and Patnaik, P. C. (1978) *Developing a Site Selection Methodology for Wind Energy Conversion Systems*, DOE/ET/20280-3, prepared for the U. S. Department of Energy by Science Applications Incorporated, La Jolla, CA.

Traci, R. M., Phillips, G. T. and Rock, K. C. (1979) *Wind Energy Siting Methodology Windfield Model Verification Program: I. Oahu, Hawaii Data Set*, DOE/ET/20280793, prepared for the U. S. Department of Energy by Science Applications Incorporated, La Jolla, CA.

Troen, I. and de Baas, A. (1986) "A Spectral Diagnostic Model for Wind Flow Simulation in Complex Terrain," in *Proceedings of the European Wind Energy Association Conference and Exhibition*, Rome, Italy, October 7–9, pp. 243–249.

Venkatesan, R. and Möllmann-Coers, M. (1996) "Application of a Refined Emergency Code System SPEEDI to Atmospheric Field Experiments Conducted over a Complex Terrain," *Journal of Nuclear Science and Technology*, Vol. 33, No. 2, pp. 157-165.

Venkatesan, R., Möllmann-Coers, M. and Natarajan, A. (1997) "Modeling Wind Field and Pollution Transport over a Complex Terrain Using an Emergency Dose Information Code SPEEDI," *Journal of Applied Meteorology*, Vol. 36, No. 9, pp. 1138-1159.

Walmsley, J. L., Troen, I., Lalas, D. P. and Mason, P. J. (1990) "Surface-Layer Flow in Complex Terrain: Comparison of Models and Full-Scale Observations," *Boundary-Layer Meteorology*, Vol. 52, pp. 259-281.

Weinstock, R. (1952) *Calculus of Variations*, McGraw-Hill, New York, NY, 326 pp.

Zack, J. A. and Minnich, R. A. (1991) "Integration of Geographic Information Systems with a Diagnostic Wind FIeld Model for Fire Management," *Forest Science*, Vol. 37, No. 2, pp. 560-573.

Zannetti, P. (1990) *Air Pollution Modeling: Theories, Computational Methods and Available Software*, Computational Mechanics Publications, Boston, MA, and Van Nostrand Reinhold, New York, NY.

REFERENCES ON LINEARIZED MODELS

Astrup, P., Mikkelsen, T. and Jensen, N. O. (1997) "A Fast Model for Mean and Turbulent Wind Characteristics over Terrain with Mixed Surface Roughness," *Radiation Protection Dosimetry*, Vol. 73, No. 1-4, pp. 257-260.

Astrup, P., Mikkelsen, T. and Deme, S. (2001) "METRODOS: Meteorological Preprocessor Chain," *Physics and Chemistry of the Earth, Part B: Hydrology, Oceans, and Atmosphere*, Vol. 26, No. 2, pp. 105-110.

Belcher, S. E., Xu, D. P. and Hunt, J. C. R. (1990) "The Response of a Turbulent Boundary Layer to Arbitrarily Distributed Two-Dimensional Roughness Changes," *Quarterly Journal of the Royal Meteorological Society*, Vol. 116, pp. 611-635.

Carruthers, D. J. and Choularton, T. W. (1982) "Airflow over Hills of Moderate Slope," *Quarterly Journal of the Royal Meteorological Society*, Vol. 108, pp. 603-624.

Carruthers, D. J., Hunt, J. C. R. and Weng, W. S. (1988) "A Computational Model of Stratified Turbulent Air Flow over Hills—FLOWSTAR I," *Computer Techniques in Environmental Studies: Proceedings of Envirosoft 88, 2nd International Conference*, Porto Carras, Greece, pp. 481-492.

Finardi, S., Brusasca, G., Morselli, M. G., Trombetti, F. and Tampieri, F. (1993) "Boundary-Layer Flow over Analytical Two-Dimensional Hills: A Systematic Comparison of Different Models with Wind Tunnel Data," *Boundary-Layer Meteorology*, Vol. 63, No. 3, pp. 259-291.

Hunt, J. C. R. and Richards, K. J. (1984) "Stratified Airflow over One or Two Hills," *Boundary-Layer Meteorology*, Vol. 30, pp. 223-259.

Hunt, J. C. R., Richards, K. J. and Brighton, P. W. M. (1988a) "Stably Stratified Shear Flow Over Low Hills," *Quarterly Journal of the Royal Meteorological Society*, Vol. 114, pp. 859-886.

Hunt, J. C. R., Leibovich, S., and Richards, K. J. (1988b) "Turbulent Shear Flows over Low Hills," *Quarterly Journal of the Royal Meteorological Society*, Vol. 114, pp. 1435-1470.

Hunt, J. C. R., Tampieri, F., Weng, W. S., and Carruthers, D. J. (1991) "Air Flow and Turbulence over Complex Terrain: a Colloquium and a Computational Workshop," *Journal of Fluid Mechanics*, Vol. 227, pp. 667-688.

Jackson, P. S. and Hunt, J. C. R. (1975) "Turbulent Wind Flow Over a Low Hill," *Quarterly Journal of the Royal Meteorological Society*, Vol. 101, pp. 929-955.

Mason, P. J. and Sykes, R. I. (1979) "Flow over an Isolated Hill of Moderate Slope," *Quarterly Journal of the Royal Meteorological Society*, Vol. 105, pp. 383-395.

Mason, P. J. and King, J. C. (1985) "Measurements and Predictions of Flow and Turbulence over an Isolated Hill of Moderate Slope," *Quarterly Journal of the Royal Meteorological Society*, Vol. 111, pp. 617–640.

Mikkelsen, T., Thykier-Nielsen, S., Astrup, P., Santabárbara, M., Sørensen, J. H., Rasmussen, A., Robertson, L., Ullerstig, A., Deme, S., Martens, R., Bartzis, J. G. and Päsler-Sauer, J. (1997) "MET-RODOS: A Comprehensive Atmospheric Dispersion Module," *Radiation Protection Dosimetry*, Vol. 73, Nos. 1-4, pp. 45-56.

Snyder, W. H., Thompson, R. S., Eskridge, R. E., Lawson, R. E., Castro, I. P., Lee, J. T., Hunt, J. C. R. and Ogawa, Y. (1985) "The Structure of Strongly Stratified Flow over Hills: Dividing-Streamline Concept," *Journal of Fluid Mechanics*, Vol. 152, pp. 249-288.

Sokolnikoff, I. S. and Redheffer, R. M. (1966) *Mathematics of Physics and Modern Engineering*, McGraw-Hill, 752 pp.

Taylor, P. A. (1977) "Numerical Studies of Neutrally Stratified Planetary Boundary-Layer Flow above Gentle Topography I: Two-Dimensional Cases," *Boundary-Layer Meteorology*, Vol. 12, No. 1, pp. 37-60.

Taylor, P. A. and Walmsley, J. L. (1981) "Estimates of Wind-Speed Perturbation in Boundary-Layer Flow over Isolated Hills—A Challenge," *Boundary-Layer Meteorology*, Vol. 20, pp. 253-257.

Taylor, P. A., Walmsley, J. L. and Salmon, J. R. (1983) "A Simple Model of Neutrally Stratified Boundary-Layer Flow over Real Terrain Incorporating Wavenumber-Dependent Scaling," *Boundary-Layer Meteorology*, Vol. 26, No. 2, pp. 169-189.

Troen, I. and de Baas, A. (1986) "A Spectral Diagnostic Model for Wind Flow Simulation in Complex Terrain," in *Proceedings of the European Wind Energy Association Conference and Exhibition*, Rome, Italy, October 7–9, pp. 243–249.

Walmsley, J. L. and Taylor, P. A. (1981) "Estimates of Wind-Speed Perturbation in Boundary-Layer Flow over Isolated Low Hills—Solutions," *Boundary-Layer Meteorology*, Vol. 20, pp. 391-395.

Walmsley, J. L., Salmon, J. R. and Taylor, P. A. (1982) "On the Application of a Model of Boundary-Layer Flow Over Low Hills to Real Terrain," *Boundary Layer Meteorology*, Vol. 23, pp. 17-46.

Walmsley, J. L., Taylor, P. A. and Keith, T. (1986) "A Simplified Model of Neutrally Stratified Boundary-Layer Flow over Complex Terrain with Surface Roughness Modulations (MS3DJH/3R)," *Boundary-Layer Meteorology*, Vol. 36, pp. 157-186.

Walmsley, J. L., Troen, I., Lalas, D. P. and Mason, P. J. (1990) "Surface-Layer Flow in Complex Terrain: Comparison of Models and Full-Scale Observations," *Boundary-Layer Meteorology*, Vol. 52, pp. 259-281.

APPENDIX A: Fourier Decomposition

Let $F(x,z)$ denote one of the unknown perturbation functions in the linearized analysis of §3, and $F(k,z)$ its Fourier transform with respect to the x coordinate. We will use the following definitions of the transform and its inverse:

$$F(k,z) = \frac{1}{\sqrt{2\pi}}\int_{-\infty}^{\infty} F(x,z)e^{-ikx}dx \tag{51a}$$

$$F(x,z) = \frac{1}{\sqrt{2\pi}}\int_{-\infty}^{\infty} F(k,z)e^{ikx}dk \tag{51b}$$

Here $i = \sqrt{-1}$ is not to be confused with the integer coordinate index used in the main text. The quantity k is termed the *wavenumber* with respect to the x direction, and varies over a continuum of values. From Eq. (51b), $F(k,z)$ may be thought of as the (complex) amplitude of the k^{th} Fourier component of $F(x,z)$.

The above transform pair is often used in the solution of linear differential equations. Consider what happens when the transform in Eq. (51a) is applied to the first derivative of F:

$$\frac{1}{\sqrt{2\pi}}\int_{-\infty}^{\infty} e^{-ikx}\left(\frac{dF}{dx}\right)dx = \frac{1}{\sqrt{2\pi}}\left[F(x,z)e^{-ikx}\Big|_{-\infty}^{\infty} + ik\int_{-\infty}^{\infty} F(x,z)e^{-ikx}dx\right]$$

$$= 0 \text{ if } F(\pm\infty, z) = 0$$

$$= ikF(k,z)$$

The first equality results from an integration by parts. The second assumes that all perturbations vanish at $\pm\infty$. An analogous procedure, involving two successive integrations by parts with respect to x, shows that the second derivative, d^2F/dx^2, transforms according to,

$$\frac{d^2}{dx^2}F(x,z) \rightarrow -k^2F(k,z)$$

provided that both F and dF/dx vanish at $x = \pm\infty$. And in general, the n^{th} derivative of F, after n successive integrations by parts, can be shown to transform to,

$$\frac{d^n}{dx^n}F(x,z) \rightarrow (ik)^nF(k,z) \qquad \text{for all } n \geq 0 \tag{52}$$

provided that F and each of its derivatives through $d^{(n-1)}F/dx^{(n-1)}$ vanish at $x = \pm\infty$. (It is understood that $d^{(0)}F/dx^{(0)} \equiv F$.) Hence, when applied to a linear differential equation, the transform in Eq. (51a) results in F being replaced by F, and any differential operations with respect to x with an algebraic dependence on the wavenumber k. This is the reason Jackson and Hunt (1975) assume that the hill is isolated—so that all the "boundary terms" vanish (*cf.* p. 40).

The preceding arguments carry over readily to the three-dimensional case, by generalizing F to $F(x,y,z)$. The Fourier transform is applied to the linearized equations with respect to both horizontal coordinates, x and y. Provided F and its derivatives all disappear as either x or $y \to \pm\infty$, the result is that any differential operations with respect to x or y are eliminated, and replaced by algebraic functions of k_1 and k_2. The latter denote the wavenumbers in the x and y directions, respectively. The unknown F is transformed to $F(k_1,k_2,z)$—the (complex) amplitude of the $(k_1,k_2)^{\text{th}}$ Fourier component in the horizontal decomposition—in what is now a system of ordinary differential equations in z.

In applying these concepts to real terrain, it is necessary to think of the region of interest — and the resulting flow—as being repeated periodically in one (if 2D) or both (if 3D) horizontal coordinates. In that case the integrals in Eqs. (51a)-(51b) are no longer defined. Rather than use transforms, such periodic variations are best analyzed using Fourier series. The coefficients for the complex Fourier series of a function $F(x,z)$ with period $2L$ in x are given by (see *e.g.*, Sokolnikoff and Redheffer (1966), Chapter 1, p. 71),

$$F_m(z) = \frac{1}{L}\int_{-L/2}^{L/2} F(x,z)e^{-i\left(\frac{2\pi m}{L}\right)x}dx \qquad \text{for } m = 0, \pm1, \pm2, \ldots \tag{53a}$$

and the series itself is:

$$F(x,z) = \sum_{m=-\infty}^{\infty} F_m(z)e^{i\left(\frac{2\pi m}{L}\right)x} \tag{53b}$$

Comparing these to Eqs. (51a)-(51b), we see that the wavenumber k is replaced by the grouping $2\pi m/L$, and the latter, instead of varying over a continuum of values, can take on only those discrete values dictated by m being an integer between $\pm\infty$. For this reason, F is now written as $F_m(z)$ rather than $F(m,z)$, to emphasize that it represents a set of coefficients, each of which is a function of z.

The above pair of equations is useful in solving linear differential equations for which the solutions F are know to be periodic. Consider what happens when the integral operator in Eq. (53a) is applied to the first derivative of F:

$$\frac{1}{L}\int_{-L/2}^{L/2} e^{-i\left(\frac{2\pi m}{L}\right)x}\frac{dF}{dx}dx = \frac{1}{L}\left[F(x,z)e^{-i\left(\frac{2\pi m}{L}\right)x}\Big|_{-L/2}^{L/2} + i\left(\frac{2\pi m}{L}\right)\int_{-L/2}^{L/2} F(x,z)e^{-i\left(\frac{2\pi m}{L}\right)x}dx\right]$$

$$= \frac{1}{L}\left[F(L/2,z)e^{-im\pi} - F(-L/2,z)e^{im\pi}\right] + i\left(\frac{2\pi m}{L}\right)F_m(z)$$

where again an integration by parts was used. But $e^{-im\pi} = e^{im\pi} = (-1)^m$, so the above reduces to,

$$\frac{1}{L}\int_{-L/2}^{L/2} e^{-i\left(\frac{2\pi m}{L}\right)x}\frac{dF}{dx}dx = \frac{1}{L}\underbrace{\left[F(L/2,z)-F(-L/2,z)\right]}_{=0}(-1)^m + i\left(\frac{2\pi m}{L}\right)F_m(z)$$

$$= i\left(\frac{2\pi m}{L}\right)F_m(z)$$

Similarly, if the same operation is applied to d^2F/dx^2, two successive integrations by parts and the fact that dF/dx is also periodic will show that the second-order derivative transforms according to:

$$\frac{d^2}{dx^2}F(x,z) \rightarrow -\left(\frac{2\pi m}{L}\right)^2 F_m(z)$$

and in general, the n^{th}-order derivative with respect to x will be transformed to

$$\frac{d^n}{dx^n}F(x,z) \rightarrow \left(i\frac{2\pi m}{L}\right)^n F_m(z) \qquad \text{for all } n \geq 0 \tag{54}$$

assuming that F and all derivatives up through $d^{(n-1)}F/dx^{(n-1)}$ have periodicity L. Note the similarity between this result and Eq. (52). Thus, when periodic solutions are involved, the integral operator in Eq. (53a) has an effect on linear differential equations analogous to the effect that Eq. (51a) has for isolated disturbances, *viz.*, F is replaced by F_m and any differential operations with respect to x are replaced with algebraic functions of $(2\pi m/L)$. These concepts also carry over readily to more than one horizontal coordinate.

Intentionally Left Blank

Distribution

1	MS 1393	B. A. Boughton	Org. 5800
7	MS 0767	W. G. Rhodes, III	Org. 5817
1	MS 0767	J. D. Fulton	Org. 5817
4	MS 0767	W. Wente	Org. 5817
1	MS 0783	M. E. Larsen	Org. 5854
1	MS 0841	T. C. Bickel	Org. 9100
1	MS 0824	A. C. Ratzel	Org. 9110
1	MS 0834	M. R. Prairie	Org. 9112
1	MS 0826	W. L. Hermina	Org. 9113
1	MS 0834	J. E. Johannes	Org. 9114
1	MS 0836	E. S. Hertel	Org. 9116
1	MS 0836	R. O. Griffith	Org. 9117
1	MS 0836	J. E. Brockmann	Org. 9117
1	MS 0836	C. E. Hickox	Org. 9117
1	MS 1135	L. A. Gritzo	Org. 9132
1	MS 0835	J. M. McGlaun	Org. 9140
1	MS 0835	S. N. Kempka	Org. 9141
5	MS 0835	G. F. Homicz	Org. 9141
1	MS 0835	J. H. Strickland	Org. 9141

1	MS 9018	Central Technical Files	Org. 8945-1
2	MS 0899	Technical Library	Org. 9616
1	MS 0612	Review & Approval Desk For DOE/OSTI	Org. 9612

Intentionally Left Blank